DISCUSSION PAPER SERIES

DP17134

Local Projections in Unstable Environments: How Effective is Fiscal Policy?

Atsushi Inoue, Barbara Rossi and Yiru Wang

MONETARY ECONOMICS AND FLUCTUATIONS

CEPR

ISSN 0265-8003

Local Projections in Unstable Environments: How Effective is Fiscal Policy?

Atsushi Inoue, Barbara Rossi and Yiru Wang

Discussion Paper DP17134
Published 24 March 2022
Submitted 23 March 2022

Centre for Economic Policy Research
33 Great Sutton Street, London EC1V 0DX, UK
Tel: +44 (0)20 7183 8801
www.cepr.org

This Discussion Paper is issued under the auspices of the Centre's research programmes:

- Monetary Economics and Fluctuations

Local Projections in Unstable Environments: How Effective is Fiscal Policy?

Abstract

The paper develops a local projection estimator for estimating impulse responses in the presence of time variation. Importantly, we allow local instabilities in both slope coefficients and variances. Monte Carlo simulations illustrate that the method performs well in practice. Using our proposed estimator, we shed new light on the effects of fiscal policy shocks and the size of government spending multipliers. Our analysis uncovers the existence of instabilities that were unaccounted for in previous studies, and links time variation in the multipliers to the size of government debt.

JEL Classification: C22, C26, C32, C36, C53

Keywords: Time variation, local projections, Instability, Path Estimator, Weighted Average Risk, Fiscal policy, Fiscal Multiplier, monetary policy, government spending

Atsushi Inoue - atsushi.inoue@vanderbilt.edu
Vanderbilt University

Barbara Rossi - barbara.rossi@upf.edu
ICREA-Universitat Pompeu Fabra, Univ. Pompeu Fabra, ICREA, Barcelona School of Economics, CREI and CEPR

Yiru Wang - yiru.wang@pitt.edu
University of Pittsburgh

Acknowledgements
We thank conference participants at RCEA conference on recent developments in economics, econometrics and finance (2022), Bundesbank forecasting workshop (2022), EEA-ESEM (2021), IAAE (2021), Armenian Economic Association Meetings (2021), SIdE-IEA 8th WEEE (2020), as well as seminar participants at Universitat of Pompeu Fabra and University of Vienna. Part of this work is based on the third chapter of Yiru Wang's Ph.D. dissertation at Universitat of Pompeu Fabra in 2019. This publication has been supported by the Spanish Ministry of Science and Innovation, under grant PID2019-107352GB-I00. Barbara Rossi acknowledges financial support from the Spanish Agencia Estatal de Investigacion (AEI), through the Severo Ochoa Programme for Centres of Excellence in R&D (Barcelona School of Economics CEX2019-000915-S).

Local Projections in Unstable Environments: How Effective is Fiscal Policy?*

Atsushi Inoue† Barbara Rossi‡ Yiru Wang§

This version: March 14, 2022

Abstract

This paper develops a local projection estimator for estimating impulse responses in the presence of time variation. Importantly, we allow local instabilities in both slope coefficients and variances. Monte Carlo simulations illustrate that the method performs well in practice. Using our proposed estimator, we shed new light on the effects of fiscal policy shocks and the size of government spending multipliers. Our analysis uncovers the existence of instabilities that were unaccounted for in previous studies, and links time variation in the multipliers to the size of government debt.

J.E.L. Codes: C22, C26, C32, C36, C53

Keywords: Time variation, Local Projections, Instability, Path Estimator, Weighted Average Risk, Fiscal Policy, Fiscal Multiplier, Monetary Policy, Government Spending

*We thank conference participants at RCEA conference on recent developments in economics, econometrics and finance (2022), Bundesbank forecasting workshop (2022), EEA-ESEM (2021), IAAE (2021), Armenian Economic Association Meetings (2021), SIdE-IEA 8th WEEE (2020), as well as seminar participants at Universitat of Pompeu Fabra and University of Vienna. Part of this work is based on the third chapter of Yiru Wang's Ph.D. dissertation at Universitat of Pompeu Fabra in 2019. This publication has been supported by the Spanish Ministry of Science and Innovation, under grant PID2019-107352GB-I00. Barbara Rossi acknowledges financial support from the Spanish Agencia Estatal de Investigación (AEI), through the Severo Ochoa Programme for Centres of Excellence in R&D (Barcelona School of Economics CEX2019-000915-S).

†Department of Economics, Vanderbilt University, VU Station B, Box #351819, 2301 Vanderbilt Place, Nashville, TN 37235, USA. E-mail: atsushi.inoue@vanderbilt.edu.

‡ICREA-Universitat of Pompeu Fabra, Barcelona School of Economics and CREI, c/Ramon Trias Fargas 25/27, Barcelona 08005, Spain. E-mail: barbara.rossi@upf.edu.

§Department of Economics, University of Pittsburgh, Wesley Posvar Hall, 230 South Bouquet Street, Pittsburgh, PA 15260. E-mail: yiru.wang@pitt.edu.

1 Introduction

This paper proposes a local projection-based estimator for time-varying parameter models, which we refer to as the "time-varying parameter local projection"estimator (or TVP-LP in short). We show how to estimate the parameters of the model as well as the associated impulse response functions.

Impulse responses are an important tool in empirical macroeconomic analyses for estimating the effects of unanticipated structural disturbances on the economy. Impulse responses are often estimated by recursively iterating Vector Autoregressions (VARs) – see Sims (1980) and Stock and Watson (2016), or VARs with external instruments (Montiel Olea, Stock and Watson 2021). In the presence of instabilities, which are widespread in recent economic data, researchers rely on time-varying parameter Vector Autoregressions (TVP-VARs); see, for instance, Canova (1993), Cogley and Sargent (2005), Primiceri (2005), and Clark (2011). VARs, however, are not robust to the presence of non-invertibility due to omitted variables and misspecification - see Stock and Watson (2018).

An increasingly widespread alternative to estimating VARs and their impulse responses is the local projection approach by Jordà (2005). The idea behind local projections is to project future outcomes on current covariates for each forecast horizon. The relationship between VARs with local projections has been investigated in Montiel Olea and Plagborg-Møller (2021). Local projections are robust to non-invertibility and also greatly simplify estimation in the presence of non-linearities and panel data - see Jordà (2020) for a review. However, local projection estimators typically assume stable environments.

In this paper, we propose an estimator for local projections and their impulse response functions in unstable environments, allowing for a stochastic evolution of the parameters over time. Thus, our work is the counterpart to time-varying parameter VARs in a local projection framework. The methodology that we propose has widespread applicability since there is substantial evidence of instabilities in macroeconomic models.

While it is possible to estimate local projections allowing for instabilities using state-dependent

models, as in Auerbach and Gorodnichenko (2012), Fazzari, Morley and Panovska (2015), Ramey and Zubairy (2018), and Barnichon, Debortoli and Matthes (2021), these approaches only allow for discrete shifts in the models' parameters, linked to the presence of observable state variables. Finally, Cloyne, Jordà and Taylor (2021) argue that the way fiscal multipliers vary over time depends on both monetary policy as well as the macroeconomic environment. One of the advantages of our estimator is that it allows for more flexible forms of time variation than state dependence. Thus, it can be used to guide researchers in identifying potentially important instabilities and their determinants.

From an estimation standpoint, this paper introduces local time variation in the local projections framework. In particular, we consider parameter paths whose variability is of order of magnitude $T^{-1/2}$ following Condition 2 in Müller and Petalas (2010), which accommodates a wide range of parameter instabilities, such as random walk variability occurring in either the full sample or part of the sample, piece-wise constant paths with finitely many jumps, and so on. Importantly, the local time variation is allowed in both coefficients and variances, thus allowing researchers to model and estimate changes in both structural shocks' volatility and their transmission mechanism. Documenting the time variation in impulse responses is useful for several purposes. First, the path estimators themselves describe the parameter evolution over time and shed light on the potential sources of instability. Second, the time-varying parameter local projections quantify how macroeconomic variables respond to structural shocks at different points in time, allowing for potentially different transmission mechanisms under different economic conditions. Third, the endpoint of the parameter path is useful for forecasting.

The methodology introduced in this paper builds on the path estimator introduced by Müller and Petalas (2010), who consider an unstable time series model with a log-likelihood function of the form $\sum_{t=1}^{T} l_t(\theta_t) = \sum_{t=1}^{T} l_t(\theta+\delta_t)$, while its corresponding stationary model has the same likelihood with time-invariant parameters $\theta \in \Theta \subset \mathbb{R}^q$. They derive asymptotically weighted average risk (WAR) minimizing path estimators for $\{\theta_t\}_{t=1}^{T}$ and weighted average power (WAP) maximizing parameter stability test statistics, assuming an approximately stationary model and a weighting

function for the variability $\{\delta_t\}_{t=1}^T$ that is a (demeaned) multivariate Gaussian random walk. The covariance matrix of the approximate posterior of the path estimators is a WAR minimizing interval estimator that measures the accuracy of the path estimators. We differ from their work as we focus on a local projection setting and allow for different magnitude of time variation for different blocks of parameters.

Methodologically, our TVP-LP contributes to the existing LP literature in the following ways. First, the TVP-LP builds on the method of local projections by Jordà (2005), hence the impulse responses are based on a direct multi-step forecasting regression at each forecast horizon, rather than iterating a VAR model into increasingly distant horizons. The equivalence between Jordà's (2005) local projections and VARs has been studied by Montiel Olea and Plagborg-Møller (2021), although their analysis excludes the existence of time-varying parameters. Thus, relative to (B)VARs and TVP-(B)VARs, our approach preserves the advantages of local projections – that is, it can be less sensitive to model misspecification (i.e., insufficient lag length) and non-invertibility, it accommodates highly nonlinear and flexible specifications, and has a simple and intuitive interpretation. We also extend the analysis of VARs with exogenous variables (Montiel Olea, Stock and Watson 2021) to time-varying environments.

Second, the TVP-LP method also differs from traditional local projections and their extensions, which, unlike our study, are all based on constant environments: Barnichon and Brownlees (2019) propose smooth local projections using B-spline smoothing, which substantially increases precision over local projections, while Miranda-Agrippino and Ricco (2021) propose a Bayesian approach to local projections as an alternative to BVARs. Our proposed method differs from theirs as it assumes an unstable environment and allows for time variation in the parameters.

Third, compared with other VAR/LP-based models considering time variation (such as TVP-(B)VAR, state-dependent LPs, etc), our approach does not require specifying parametrically the exact form of the instability process. Thus, it allows for more flexible forms of time variation such as structural breaks, linear trends, stochastic trends occurring in sub-samples, and piece-wise constant paths with finitely many jumps. This is a feature distinct from Ruisi's (2019) Bayesian

proposal of time-vayring local projections in his recent paper.

Using our approach, we study whether there are instabilities in government spending multipliers that are still unaccounted for in the existing literature. In particular, while the debate in the literature focuses on whether the effects of fiscal policy depend on the state of the economy (Fazzari, Morley and Panovska 2015, 2021) or on the existence of the zero lower bound (Ramey and Zubairy 2018) or the interaction between fiscal and monetary policy (Cloyne, Jordà and Taylor 2021) or even other variables (e.g., Goemans (2022) uses uncertainty), we allow for more general and agnostic forms of time variation. This generality, possible because of our methodology, has the potential to uncover other instabilities that may help reconcile the wide range of estimates of government spending multipliers, ranging from 0.8 to 7.5 (Ramey 2011b). Our findings can be summarized as follows. First, both government spending and GDP responses to a government spending shock exhibit heterogeneity across time, and so do cumulative spending multipliers. Importantly, and surprisingly, the pattern of both the responses and the multipliers are sometimes the opposite of state-dependent models, thus implying that the amount of slack in the economy is not the only factor influencing the magnitude of the effect of a spending stimulus. Overall, our results suggest that the TVP-LP responses contain richer information, and can better characterize instabilities, than linear or state-dependent models.

The remainder of this paper is organized as follows. Section 2 discusses the TVP-LP framework and the impulse response estimation methodology. Section 3 discusses time-varying VARs and LPs with external instruments. Section 4 presents Monte Carlo simulations calibrated on Primiceri's (2005) structural VAR (SVAR) model. Section 5 presents our empirical evidence on government spending multipliers and responses to a fiscal policy shock using our TVP-LP method. Section 6 concludes.

2 Impulse Responses under Unstable Local Projections

Let Y_t, a $(K \times 1)$ vector of macroeconomic variables, be written in terms of current and past shocks ϵ_t in a structural moving average representation:

$$Y_t = \Theta(L)\epsilon_t, \tag{1}$$

where L denotes the lag operator, $\Theta(L) \equiv \Theta_0 + \Theta_1 L + \Theta_2 L^2 + \cdots$, and Θ_h is a $(K \times K)$ matrix of coefficients. The structural shocks are assumed to be independent and identically distributed with diagonal covariance matrix $E[\epsilon_t \epsilon_t'] = \Sigma_\epsilon$.

The coefficients of $\Theta(L)$ are the structural impulse responses, i.e., the dynamic causal effects of the structural shocks. To be more specific and without loss of generality, suppose we focus on the first shock, $\epsilon_{1,t}$. The effect of a unit increase in $\epsilon_{1,t}$ on the value of the second variable, $Y_{2,t}$, is $\Theta_{h,21}$, which can be rewritten as:

$$\Theta_{h,21} = E[Y_{2,t+h}|\epsilon_{1,t} = 1, \epsilon_{2:K,t}, \epsilon_s, s \neq t] - E[Y_{2,t+h}|\epsilon_{1,t} = 0, \epsilon_{2:K,t}, \epsilon_s, s \neq t], \qquad h = 0, 1, \cdots. \tag{2}$$

Following Stock and Watson (2016), we assume the unit effect normalization $\Theta_{0,11} = 1$.

The impulse response coefficient in eq.(2) can be calculated either by recursively iterating a model to characterize the structure of successive observations (e.g., by recursively iterating VARs), or via direct linear regressions of future outcomes on current covariates for each forecast horizon (i.e., Jordà's (2005) local projections). In the latter, the impulse response coefficient in eq.(2) can be obtained by estimating the following local projection regression:

$$Y_{2,t+h} = \Theta_{h,21}\epsilon_{1,t} + \gamma_h' W_t + u^h_{2,t+h}, \qquad h = 0, 1, \cdots, \tag{3}$$

where W_t denotes the control variables (including lagged values of Y_t) and the residual $u^h_{2,t+h}$ is a linear combination of the shocks $\{\epsilon_{t+h}, \cdots, \epsilon_{t+1}, \epsilon_{2:K,t}\}$,[1] thus serially correlated. The intercept

[1]The subscript '$i:j$' denotes the i-th to the j-th elements (rows or columns) of a vector (matrix).

term is omitted for notational simplicity and without loss of generality.

Let $f(Y_{2,t+h}|\epsilon_{1,t}, W_t, \theta)$ denote a family of conditional density functions for $Y_{2,t+h}$ under the assumption that $\{u^h_{2,t+h}\}$ has zero mean and variance σ_u^2, where θ is a $(q \times 1)$ vector including all the parameters of interest for a certain horizon h, $h = 0, 1, \cdots$, and $\theta \in \mathbf{\Theta} \subset \mathbb{R}^q$. For example, $\theta = (\Theta_{h,21}, \gamma_h', \ln \sigma_u)'$ when estimating eq.(3) for a given h or $\theta = (\Theta_{0,21}, \Theta_{1,21}, \cdots, \Theta_{H,21}, \gamma_0', \cdots, \gamma_H', \ln \sigma_u)'$ when estimating eq.(3) for $h = 0, 1, \cdots, H$. In the local projections framework, $\sum_{t=1}^T l_t(\theta), l_t(\theta) = \ln f(Y_{2,t+h}|\epsilon_{1,t}, W_t, \theta)$, is not the correct log-likelihood function as the error terms in the local projections are serially correlated. Let θ_0 denote the vector that consists of the true conditional mean parameter values (e.g., $\Theta_{h,21}$ and γ_h in the first example above) and the pseudo-true volatility parameter values (e.g., σ_u^2 in the previous example). Even with serially correlated error terms, the maximum likelihood estimation (MLE) consistently estimates θ_0 with a "sandwich"asymptotic covariance matrix – see White (1982) and Levine (1983). In particular, let $s_t(\theta) = \partial l_t(\theta)/\partial\theta, t = 1, \ldots, T$ denote the sequence of $(q \times 1)$ score vectors, let $h_t(\theta) = -\partial s_t(\theta)/\partial\theta, t = 1, \ldots, T$, denote the sequence of $(q \times q)$ Hessians. Then, $\sqrt{T}(\widehat{\theta} - \theta_0) \Rightarrow \mathcal{N}(0, S)$, where the sandwich matrix S is typically estimated as $\widehat{S} = \widehat{H}^{-1}\widehat{V}\widehat{H}^{-1}$ and $\widehat{H} = \frac{1}{T}\sum_{t=1}^T h_t(\widehat{\theta})$. If the score vectors are i.i.d., then $\widehat{V} = \frac{1}{T}\sum_{t=1}^T s_t(\widehat{\theta})s_t(\widehat{\theta})'$; however, in this context, the residuals in eq.(3) are serially correlated, thus HAC estimators, such as Newey and West's (1987) estimator, may be used to account for the serial correlation.[2] Thus, eq.(3) is a stationary system of local projections with a (mis)specified log-likelihood function of the form $\sum_{t=1}^T l_t(\theta)$.

Now consider the corresponding time-varying parameter local projection, which has the same likelihood $\sum_{t=1}^T l_t(\cdot)$ as the stationary local projection in eq.(3) but with time-varying parameters

[2]Apart from using HAC estimators, an alternative way to correct for the autocorrelation in the error term is to include the residuals in the regression, see Lusompa (2021). Then, eq.(3) can be written as

$$Y_{2,t+h} = \Theta_{h,21}\epsilon_{1,t} + \gamma_h'\widetilde{W}_t + u_{2,t+h}, \qquad h = 0, 1, \cdots,$$

where $u_{2,t+h}$ denotes the reduced-form error term at period $t+h$, and $\widetilde{W}_t$ includes current and past values of $Y_{1,t-i}, i = 1, 2, \cdots, Y_{2,t-j}, j = 0, 1, 2, \cdots$, as well as the other reduced-form error terms $u_{\cdot,t+1}, \cdots, u_{\cdot,t+h-1}$. Due to $u_{\cdot,t+1}, \cdots, u_{\cdot,t+h-1}$ being unobserved, the estimates from the VAR must be used instead. Lusompa (2021) shows that estimates of the impulse responses are still consistent using estimated residuals. The error term $u_{2,t+h}$ is thus serially uncorrelated. In this case, define $\theta = (\Theta_{h,21}, \gamma_h', \ln \sigma_u)'$.

$\{\theta_t\}_{t=1}^T = \{\theta + \delta_t\}_{t=1}^T$:

$$Y_{2,t+h} = \Theta_{h,21,t}\epsilon_{1,t} + \gamma_{h,t}' W_t + u_{2,t+h}^h, \qquad h = 0, 1, \cdots, \tag{4}$$

where $\Theta_{h,21,t}$, $\gamma_{h,t}$, and $\sigma_{u,t+h}^2$ are the time-varying analogs of $\Theta_{h,21}$, γ_h, and σ_u^2 in eq.(3) for each horizon $h = 0, 1, \cdots$.

As shown in Müller and Petalas (2010), the sample information about θ and $\{\delta_t\}_{t=1}^T$ is approximately independent and described by the pseudo model:

$$\begin{aligned} \widehat{\theta} &= \theta + T^{-1/2}\widehat{S}\nu_0, \\ \widehat{H}\widehat{V}^{-1}s_t(\widehat{\theta}) &= \widehat{S}^{-1}\delta_t + \nu_t, \quad t = 1, \cdots, T, \end{aligned} \tag{5}$$

with $\nu_t \overset{\text{i.i.d.}}{\sim} \mathcal{N}(0, \widehat{H})$. Here, $\widehat{H}$, $\widehat{V}$, and $\widehat{S}$ are consistent estimators of the counterparts defined above. Due to model misspecification, there is a discrepancy between $\widehat{\theta} \sim \mathcal{N}(\theta_0, \widehat{H}^{-1}/T)$ and the approximate sampling distribution $\widehat{\theta} \sim \mathcal{N}(\theta_0, \widehat{S}/T)$, and as shown in Müller (2013), the latter should be used for inference on the pseudo-true parameters.

Assuming an approximately stationary model and a weighting function for $\{\delta_t\}_{t=1}^T$ that is a demeaned multivariate Gaussian random walk, Müller and Petalas (2010) derive asymptotically WAR minimizing path estimators $\{\widehat{\theta}_t\}_{t=1}^T$:

1. For $t = 1, \ldots, T$, let x_t and $\tilde{y}_t$ be all the elements of $\widehat{H}^{-1}s_t(\widehat{\theta})$ and $\widehat{H}\widehat{V}^{-1}s_t(\widehat{\theta})$, respectively.

2. For $c_i \in C = \{0, c_1, c_2, \cdots, c_{n_G}\}$,[3] $i = 0, 1, \cdots, n_G$, compute

   (a) $r_i = 1 - \frac{c_i}{T}$, $z_{i,1} = x_1$, and $z_{i,t} = r_i z_{i,t-1} + x_t - x_{t-1}, t = 2, \ldots, T$;

   (b) the residuals of $\{\tilde{z}_{i,t}\}_{t=1}^T$ of a linear regression of $\{z_{i,t}\}_{t=1}^T$ on $\{r_i^{t-1}I_q\}_{t=1}^T$;

   (c) $\overline{z}_{i,T} = \tilde{z}_{i,T}$, and $\overline{z}_{i,t} = r_i\overline{z}_{i,t+1} + \tilde{z}_{i,t} - \tilde{z}_{i,t+1}, t = 1, \ldots, T-1$;

[3] For the factor of proportionality $\frac{c^2}{T^2}$, Müller and Petalas (2010) suggest a default choice of minimizing WAR relative to an equal-probability mixture of $c \in \{0, 5, 10, \ldots, 50\}$, which represents the standard deviation of the end point of the random walk weighting function and covers a wide range of magnitudes for the time variation. The extension to allow vector c_i and matrix C is further described in the Not-for-Publication Appendix A.

(d) $\{\widehat{\theta}_{i,t}\}_{t=1}^{T} = \{\widehat{\theta} + x_t - r_i\overline{z}_{i,t}\}_{t=1}^{T}$;

(e) $qLL(c_i) = \sum_{t=1}^{T}(r_i\overline{z}_{i,t} - x_t)'\tilde{y}_t$ and $\tilde{w}_i = \sqrt{T(1-r_i^2)r_i^{T-1}/((1-r_i^{2T}))}exp[-\frac{1}{2}qLL(c_i)]$ (set $\tilde{w}_0 = 1$).

3. Compute $w_i = \tilde{w}_i / \sum_{j=0}^{n_G}\tilde{w}_j$.

4. The parameter path estimator is given by $\{\widehat{\theta}_t\}_{t=1}^{T} = \{\sum_{j=0}^{n_G} w_i\widehat{\theta}_{i,t}\}_{t=1}^{T}$.

With the weighting functions for $\{\delta_t\}_{t=1}^{T}$ and θ interpreted as priors from a Bayesian perspective, the approximate posterior for θ_t is a mixture of multivariate normals $\mathcal{N}\left(\widehat{\theta}_{i,t}, T^{-1}\widehat{S}\kappa_t(c_i)\right), i = 0,\ldots,n_G$ with mixing probabilities w_i where $\widehat{S} = \widehat{H}^{-1}\widehat{V}\widehat{H}^{-1}$, $\kappa_t(c) = \frac{c(1+e^{2c}+e^{2ct/T}+e^{2c(1-t/T)})}{2e^{2c}-2}$, and $\kappa_t(0) = 1$, see Müller and Petalas (2010) for more details. Following their results, we approximate the mixture of normals by $N(\widehat{\theta}_t, \Omega_t)$ where $\Omega_t = \sum_{i=0}^{n_G} w_i\left(T^{-1}\widehat{S}\kappa_t(c_i) + (\widehat{\theta}_{i,t} - \widehat{\theta}_t)(\widehat{\theta}_{i,t} - \widehat{\theta}_t)'\right)$. Thus, the confidence interval $\left[\widehat{\theta}_{t,j} - 1.96\sqrt{\Omega_{t,jj}}, \widehat{\theta}_{t,j} + 1.96\sqrt{\Omega_{t,jj}}\right]$ with $\widehat{\theta}_{t,j}$ the j-th element of $\widehat{\theta}_t$ and $\Omega_{t,jj}$ the (j,j) element of Ω_t is the 95% equal-tailed approximate posterior probability interval for $\theta_{t,j}$, the j-th element of θ at time t.

Thus, the impulse responses based on a TVP-LP in eq.(4) are estimated using $\widehat{\Theta}_{h,21,t}$, which is the appropriate element in the path estimators $\widehat{\theta}_t$. Furthermore, to quantify the accuracy of the impulse responses, their confidence bands can be constructed based on Ω_t, the covariance matrix of the approximate posterior for θ_t.

3 VARs and Local Projections with External Instruments and Time-varying Parameters

The framework proposed in Section 2 can also be used to obtain path estimators in the time-varying parameter local projection using external instruments (TVP-LP-IV). In addition, given the well-known relationship between local projections and VAR models (Montiel Olea and Plagborg-Møller 2021), our framework can be implemented as well in time-varying parameter (structural) VARs

(TVP-VAR or TVP-SVAR) and TVP-VARs using external instruments (TVP-VAR-IV or TVP-proxy VAR), as we discuss below.

Time-varying Parameter LP-IV (TVP-LP-IV)

Now we consider the scenario where external instruments are used, see, e.g., Ramey and Zubairy (2018), where narrative measures of fiscal policy changes are used as instruments to estimate the government spending multipliers. Consider the following TVP-LP, where the LP is defined in terms of ensemble averages at time t, with control variables W_t:

$$Y_{2,t+h} = \Theta_{h,21,t} Y_{1,t} + \gamma'_{h,t} W_t + u^h_{2,t+h} \qquad h = 0, 1, \cdots . \tag{6}$$

When $Y_{1,t}$ is endogenous (in the sense that it is correlated with $u^h_{2,t+h}$ in eq.(6)), then the OLS estimator in eq.(6) is not valid. Let z_t be a suitable instrument that satisfies both the relevance condition ($E[\epsilon_{1,t} z_t^\perp] \neq 0$) and the exogeneity condition ($E[\epsilon_{2:K,t} z_t^\perp] = 0$, $E[\epsilon_{t+s} z_t^\perp] = 0, \forall s \neq 0$). The effect of the first shock $\epsilon_{1,t}$ on the value of the second variable $Y_{2,t}$ at horizon h therefore is $\Theta_{h,21,t} = \frac{E[Y^\perp_{2,t+h} z_t^\perp]}{E[Y^\perp_{1,t} z_t^\perp]}$, where $x_t^\perp = x_t - \text{Proj}(x_t | W_t)$ for some variable x_t – see Stock and Watson (2018) and Montiel Olea, Stock and Watson (2021) for more detailed discussions of structural identification using external instruments.

To estimate impulse responses in this scenario, we consider the following reduced-form regression for $Y_t = (Y_{1,t}, Y_{2,t})'$, where W_t contains past values of Y (i.e., $Y_{t-1}, Y_{t-2}, \cdots$):

$$Y_{t+h} = \begin{bmatrix} \pi_{h,t} \\ \pi_{h,t} \Theta_{h,21,t} \end{bmatrix} z_t + \Gamma_{h,t}(L) W_t + v_{t+h} \qquad h = 0, 1, \cdots . \tag{7}$$

Let $\theta_t := \left(\pi_{h,t}, \Theta_{h,21,t}, vec\left(\Gamma_{h,t}(L)\right)', vech\left(\Sigma_{v,t+h}\right)'\right)'$ for a given h. Suppose $f(Y_{t+h} | z_t, Y_{t-1}, \cdots, Y_{t-p}, \theta_t)$ is a family of conditional density functions for Y_{t+h} under the assumption that v_{t+h} has zero mean and covariance matrix $\Sigma_{v,t+h}$. Note that we allow the parameters $\pi_{h,t}$, $\Theta_{h,21,t}$, $\Gamma_{h,t}(L)$, and $\Sigma_{v,t+h}$ to be time-varying.[4] MLE consistently estimates the parameters in eq.(7) with

[4] In the existing literature, the evolution of the parameters is commonly assumed to be (geometric) random walks

a "sandwich" asymptotic covariance matrix. The procedure introduced in Section 2 will derive asymptotically WAR minimizing path estimators $\widehat{\theta}_t$, hence the estimator $\widehat{\Theta}_{h,21,t}$, which measures the effect of the first shock $\epsilon_{1,t}$ on the value of the second variable $Y_{2,t}$ at horizon h.[5]

Time-varying Parameter VARs (TVP-VARs)

A conventional approach to obtaining the impulse responses is to estimate a reduced-form VAR and identify it to obtain the responses, $\Theta_{h,t}$. Consider a TVP-VAR model:

$$\begin{aligned} Y_t &= B_{1,t}Y_{t-1} + \cdots + B_{p,t}Y_{t-p} + u_t, \qquad u_t \sim (O, \Sigma_{u,t}), \\ B_t(L)Y_t &= u_t = \Theta_{0,t}\epsilon_t, \end{aligned} \tag{8}$$

where $B_t(L) = I - B_{1,t}L - \cdots - B_{p,t}L^p$, u_t is the $(K \times 1)$ vector of reduced-form disturbances, which is a linear combination of the $(K \times 1)$ vector of structural shocks ϵ_t. The TVP-VAR impulse response function is represented by $\Theta_t(L) = C_t(L)\Theta_{0,t}$, where $C_t(L) = B_t(L)^{-1}$.[6] The VAR identification problem consists in identifying $\Theta_{0,t}$. Impose a unit effect normalization such that the diagonal elements of $\Theta_{0,t}$ are equal to 1. Also, without loss of generality, let us consider the following triangular reduction of the covariance matrix of the reduced-form disturbance $\Sigma_{u,t}$:

$$A_t \Sigma_{u,t} A_t' = \Sigma_{\epsilon,t}\Sigma_{\epsilon,t}', \tag{9}$$

where A_t is a lower triangular matrix with diagonal elements equal to one and $\Sigma_{\epsilon,t}$ is a diagonal matrix.

Furthermore, suppose $f(Y_t|Y_{t-1}, \cdots, Y_{t-p}, \theta_t)$ is a family of conditional density functions for Y_{t+h}. Let $\theta_t := (b_t', a_t', \ln \sigma_t')'$ denote the vector containing all the time-varying parameters in the

with errors following Normal distributions; see, for example, Mumtaz and Petrova (2018):

$$\begin{aligned} z_t &= \beta_t \epsilon_{1,t} + \sigma_{v,t} v_t, \qquad v_t \sim \mathcal{N}(0,1), \\ \beta_t &= \beta_{t-1} + \sigma_\beta \eta_{\beta,t}, \qquad \eta_{\beta,t} \sim \mathcal{N}(0,1), \\ \ln \sigma_{v,t} &= \ln \sigma_{v,t-1} + \sigma_\sigma \eta_{\sigma,t}, \qquad \eta_{\sigma,t} \sim \mathcal{N}(0,1). \end{aligned}$$

[5]The limited information maximum likelihood is adopted in this framework using instruments.

[6]Note that VAR requires that the structural moving average is invertible, i.e., the invertibility assumption, which is non-trivial; while LP doesn't require this invertibility assumption.

TVP-VAR, where $b_t = vec(B_t')$, a_t contains the elements below the diagonal of A_t, and $\sigma_t = diag(\Sigma_{\epsilon,t})$.[7] Then, by applying the procedure discussed in Section 2 we obtain the asymptotically WAR minimizing path estimators $\widehat{\theta}_t$, i.e., the coefficients needed to calculate the impulse responses $\widehat{C}_t(L)\widehat{\Theta}_{0,t}$.

TVP-VARs with External Instruments

Suppose there is an external instrument z_t for the endogenous variable $Y_{1,t}$ that satisfies the relevance condition ($E[\epsilon_{1,t}z_t] \neq 0$) and the exogeneity condition ($E[\epsilon_{2:K,t}z_t] = 0$). With the unit effect normalization, the effect of the first shock $\epsilon_{1,t}$ on the value of the second variable $Y_{2,t}$ is $\Theta_{0,21,t} = \frac{E[u_{2,t}z_t]}{E[u_{1,t}z_t]}$ where $u_t = Y_t - \text{Proj}(Y_t|Y_{t-1}, Y_{t-1}, \cdots, Y_{t-p})$, which is the population estimand of the reduced-form regression below:

$$Y_t = \begin{bmatrix} \pi_t \\ \pi_t\Theta_{0,21,t} \end{bmatrix} z_t + \Gamma_t(L)Y_{t-1} + v_t, \tag{10}$$

where $Y_t = (Y_{1,t}, Y_{2,t})'$.

Let $\theta_t := \left(\pi_t, \Theta_{0,21,t}, vec\left(\Gamma_t(L)\right)', vech\left(\Sigma_{v,t}\right)'\right)'$. Suppose $f(Y_t|z_t, Y_{t-1}, \cdots, Y_{t-p}, \theta_t)$ is a family of conditional density functions for Y_t under the assumption that v_t has zero mean and covariance matrix $\Sigma_{v,t}$. MLE consistently estimates the parameters in eq.(10) with a "sandwich" asymptotic covariance matrix. The procedure in Section 2 will provide asymptotically WAR minimizing path estimators $\widehat{\theta}_t$, hence $\widehat{\Theta}_{0,21,t}$.

In summary, the responses at horizon h can be obtained via the following three steps (Stock and Watson 2018): (i) obtain $\widehat{\Theta}_{0,j1,t}$ for $j = 1, 2$ from eq.(10), noting that a unit effect normalization is imposed such that $\Theta_{0,11,t} = 1$; (ii) obtain $\widehat{C}_t(L)$ from eq.(8); (iii) obtain the effects of shock $\epsilon_{1,t}$ on all the variables by $\widehat{\Theta}_{h,\cdot 1,t} = \widehat{C}_{h,t}\widehat{\Theta}_{0,\cdot 1,t}$.

[7] The evolution of b_t, a_t, and σ_t is commonly assumed to follow (geometric) random walks in the literature, see, for example, Primiceri (2005).

4 Monte Carlo Simulation

This section reports Monte Carlo simulations to evaluate the performance of our parameter path estimator in the TVP-VAR and TVP-LP models discussed in the previous sections. Note that there is no frequentist justification for the path estimator, but it is still useful to learn and understand its frequentist properties.

4.1 The benchmark New Keynesian SVAR model

Consider a small quarterly time-varying New Keynesian structural VAR model of the U.S. economy,[8] following Primiceri (2005). Let the VAR include the following three variables: the inflation rate (π_t, the annual percentage change in a chain-weighted GDP price index), the unemployment rate (υ_t, seasonally adjusted civilian unemployment rate, all workers over age 16), and a short-term nominal interest rate (i_t, yield on the three month Treasury bill rate). The sample ranges from 1953:Q1 to 2006:Q4.[9]

Consider the following TVP-VAR:

$$\begin{bmatrix} \pi_t \\ \upsilon_t \\ i_t \end{bmatrix} = C_t + B_{1,t} \begin{bmatrix} \pi_{t-1} \\ \upsilon_{t-1} \\ i_{t-1} \end{bmatrix} + \cdots + B_{p,t} \begin{bmatrix} \pi_{t-p} \\ \upsilon_{t-p} \\ i_{t-p} \end{bmatrix} + u_t, \qquad u_t \overset{i.i.d}{\sim} \mathcal{N}(0, \Sigma_{u,t}), \tag{11}$$

where $Y_t = (\pi_t, \upsilon_t, i_t)'$. Following Primiceri (2005), we consider two lags ($p = 2$) and the triangular decomposition of $\Sigma_{u,t}$ in the TVP-VAR, defined by

$$A_t \Sigma_{u,t} A_t^{'} = \Sigma_{\epsilon,t} \Sigma_{\epsilon,t}^{'}, \tag{12}$$

[8] Stock and Watson (2001), Cogley and Sargent (2005), Primiceri (2005), and Inoue and Rossi (2011) have demonstrated the importance of taking into account instabilities in VAR models.

[9] The data are obtained from the Federal Reserve Bank of St. Louis website.

where A_t is a lower triangular matrix and $\Sigma_{\epsilon,t}$ is diagonal:

$$A_t = \begin{bmatrix} 1 & 0 & 0 \\ \alpha_{21,t} & 1 & 0 \\ \alpha_{31,t} & \alpha_{32,t} & 1 \end{bmatrix}, \qquad \Sigma_{\epsilon,t} = \begin{bmatrix} \sigma_{1,t} & 0 & 0 \\ 0 & \sigma_{2,t} & 0 \\ 0 & 0 & \sigma_{3,t} \end{bmatrix}. \tag{13}$$

It thus follows that

$$\begin{bmatrix} \pi_t \\ \upsilon_t \\ i_t \end{bmatrix} = C_t + B_{1,t} \begin{bmatrix} \pi_{t-1} \\ \upsilon_{t-1} \\ i_{t-1} \end{bmatrix} + \cdots + B_{p,t} \begin{bmatrix} \pi_{t-p} \\ \upsilon_{t-p} \\ i_{t-p} \end{bmatrix} + A_t^{-1} \Sigma_{\epsilon,t} \iota_t, \tag{14}$$

and the variance of ι_t is the identity matrix.

While in our framework, we consider two methods to obtain the impulse responses. One is to estimate the TVP-VAR in eq.(11) and iterate the TVP-VAR coefficients. The other is to adopt a TVP-LP framework. Using Plagborg-Møller and Wolf's (2021) projection arguments, it can be shown that the recursively identified structural impulses of each variable to a monetary policy shock are proportional to $\beta_{h,\cdot,t}$ in:

$$\begin{aligned} \pi_{t+h} &= c_{h,\pi,t} + \beta_{h,\pi,t} i_t + \gamma_{h,\pi\pi,t} \pi_t + \phi_{h,\pi,t}(L) Y_{t-1} + u^h_{\pi,t+h}, \\ \upsilon_{t+h} &= c_{h,\upsilon,t} + \beta_{h,\upsilon,t} i_t + \gamma_{h,\upsilon\pi,t} \pi_t + \gamma_{h,\upsilon\upsilon,t} \upsilon_t + \phi_{h,\upsilon,t}(L) Y_{t-1} + u^h_{\upsilon,t+h}, \\ i_{t+h} &= c_{h,i,t} + \beta_{h,i,t} i_t + \gamma_{h,i\pi,t} \pi_t + \gamma_{h,i\upsilon,t} \upsilon_t + \phi_{h,i,t}(L) Y_{t-1} + u^h_{i,t+h}, \end{aligned} \tag{15}$$

where $\phi_{h,\cdot,t}(L)Y_{t-1}$ includes infinitely many lags of Y_t. Note that the regression for each variable in eq.(15) controls for the contemporaneous value of the variables ordered above itself.

4.2 The TVP-VAR and the TVP-LP models: A comparison

The Elliott and Müller (2006) qLL test statistic based on the TVP-VAR model in eq.(11) rejects the null hypothesis that the parameters are time-invariant.[10] We consider the following grid of parameters in our estimation procedure: $C_B = \{0, 1, \cdots, 3\}$, $C_\alpha = \{0, 2, \cdots, 6\}$, $C_{\ln\sigma} = \{0, 3, \cdots, 15\}$ for the TVP-VAR in eq.(11) and $C_\Theta = \{0, 1, \cdots, 3\}$, $C_{\ln\sigma} = \{0, 3, \cdots, 15\}$ for the TVP-LP in eq.(15).[11] The Not-for-Publication Appendix reports robustness results to other choices of C and sample sizes.

Figure 1 compares our TVP-VAR path estimates with Primiceri's (2005) posterior mean of the standard deviations, i.e., the diagonal elements of $\Sigma_{\epsilon,t}$. The time-varying standard deviation of the identified monetary policy shocks from the interest rate equation quantifies the importance of monetary policy and its changes over time. The two estimates broadly share the same trends. Similarly to Primiceri (2005), our TVP-VAR estimate of monetary policy shocks exhibits a substantially higher variance in 1979-1983, i.e., the Volcker period, while it is less volatile as well as considerably low and constant in the post-Volcker period compared with the pre-Volcker period, implying that the Taylor rule has been a good approximation of U.S. monetary policy after the Volcker period. Our TVP-VAR monetary policy shocks estimate is smoother than Primiceri's (2005) TVP-BVAR estimate.

Figure 2 compares our TVP-VAR path estimates of the coefficient matrix $B_{1,t}$ with Primiceri's (2005) posterior mean: our TVP-VAR path estimates are more volatile than Primiceri's (2005). In particular, our estimates exhibit relatively more time variation around 1975:Q1 and 1981:Q3, dates corresponding to the NBER business cycle trough and the NBER business cycle peak, respectively. Our path estimates indicate that the estimated coefficients experience relatively more time variation under these different economic conditions.

Figure 3 plots the impulse responses of inflation, unemployment, and the interest rate to a unit monetary policy shock in a series of episodes (1975:Q1, 1981:Q3, and 1996:Q1). The figure

[10] The qLL test statistic is -178.858, which is smaller than the critical value at 1% significance level. See Lemma 2 in Elliott and Müller (2006) for the limiting distribution of the qLL test statistic.

[11] C_Θ refers to the grid for the intercept and slope parameters.

compares the responses based on Primiceri's (2005) estimates with our TVP-LP estimates and our TVP-VAR estimates.[12] Figure 4 further plots the responses with 90% confidence bands for each estimate in each episode. Figures 3-4 show that the effects of monetary policy shocks differ depending on the episode. Similarly, Figures 5-6 plot the impulse responses of inflation, unemployment, and the interest rate to a unit unemployment shock, i.e., a 1% increase in unemployment, implying that the effects of unemployment shocks also differ depending on the episode. Compared to Primiceri (2005), our TVP-LP and TVP-VAR impulse responses share similar trends most of the time, but our TVP-LP estimates point to significantly larger effects. The difference in the estimates may arise from the fact that our TVP-LP responses are robust to misspecification, and thus have the potential to uncover the true impulse responses even if the VAR is non-invertible. In addition, our TVP-LP estimates can easily accommodate situations when GDP follows a non-linear model, which are often impractical or infeasible in multivariate time-varying VAR models. Finally, our new procedure is easy to implement as it doesn't require computationally intensive MCMC algorithms.

4.3 Data generating process

Consider eqs.(11)-(14) as the true data generating process (DGP). Let $\theta_t = (b_t', \alpha_t', \ln \sigma_t')'$ be the $(q \times 1)$ parameter vector including: b_t, i.e., the elements in coefficient matrices $B_{j,t}, j = 1, \ldots, p$; α_t, i.e., the off-diagonal elements in A_t; and $\ln \sigma_t$, i.e., the log of the diagonal elements in $\Sigma_{\epsilon,t}$. Consider the following time-varying process:

$$\theta_t = \theta_{t-1} + \eta_t, \qquad \eta_t \overset{\text{i.i.d}}{\sim} \mathcal{N}\left(O, \Sigma_\eta \frac{c^2}{T^2}\right).$$

By iterating eq.(11), we obtain the corresponding TVP-LP:

$$Y_{t+h} = \Theta_{h,1,t} Y_t + \Theta_{h,2,t} Y_{t-1} + \cdots + \Theta_{h,p,t} Y_{t-p+1} + u_{t+h}^h, \tag{16}$$

[12] To smooth the impulse responses, we use a cubic spline to interpolate a sine curve over unevenly-spaced sample points.

where u_{t+h}^h is a moving average of $\{u_{t+h}, \cdots, u_{t+1}\}$. When the horizon $h = 1$, the TVP-LP in eq.(16) degenerates to the TVP-VAR in eq.(11). The intercept term is omitted for notational simplicity and without loss of generality.

Suppose we are interested in the h-step ahead impulse response function. Two estimation procedures are considered to obtain path estimators of $\Theta_{h,j,t}, j = 1, 2$.

- Procedure 1: Estimate the TVP-VAR in eq.(11) and generate the path estimator $\widehat{\theta}_t^{TVP-VAR} = (\widehat{b}_t^{TVP-VAR}; \widehat{\alpha}_t^{TVP-VAR}; \ln \widehat{\sigma}_t^{TVP-VAR})$, as well as its accuracy measurement $\widehat{\Omega}_t^{TVP-VAR}$. Then the path estimator of $\Theta_{h,j,t}, j = 1, 2$, denoted as $\widehat{\Theta}_{h,j,t}^{TVP-VAR}, j = 1, 2$, can be obtained by iterating the TVP-VAR coefficients.

- Procedure 2: Estimate the TVP-LP in eq.(16) directly and generate the path estimators of $\Theta_{h,j,t}, j = 1, 2$, denoted as $\widehat{\Theta}_{h,j,t}^{TVP-LP}, j = 1, 2$, as well as its accuracy measurement $\widehat{\Omega}_{h,t}^{TVP-LP}$. The autocorrelation in the error terms is taken into consideration by using a HAC estimator.

We consider $T \in \{240, 480\}$, $c \in \{1, 4\}$, and set the initial values $\theta_0 \overset{iid}{\sim} \mathcal{N}(0, I)$. Besides, we also consider the case where the values of c are different for different blocks of parameters such that $b_t - b_{t-1} \overset{\text{i.i.d}}{\sim} \mathcal{N}\left(O, \frac{c_b^2}{T^2} I\right)$, $\alpha_t - \alpha_{t-1} \overset{\text{i.i.d}}{\sim} \mathcal{N}\left(O, \frac{c_\alpha^2}{T^2} I\right)$, and $\ln \sigma_t - \ln \sigma_{t-1} \overset{\text{i.i.d}}{\sim} \mathcal{N}\left(O, \frac{c_{\ln\sigma}^2}{T^2} I\right)$, with $(c_b, c_\alpha, c_{\ln\sigma}) = (2, 1, 4)$, as well as different ranges $C_b, C_\alpha, C_{\ln\sigma}$, respectively.

4.4 Monte Carlo Simulation Results

We conduct 2000 Monte Carlo replications for each model specification. In each replication i, we obtain $\{\widehat{b}_t^{TVP-VAR,(i)}\}_{t=1}^T$, $\{\widehat{\alpha}_t^{TVP-VAR,(i)}\}_{t=1}^T$, $\{\ln \widehat{\sigma}_t^{TVP-VAR,(i)}\}_{t=1}^T$, $\{\widehat{\Theta}_{h,j,t}^{TVP-VAR,(i)}, j = 1, 2\}_{t=1}^T$, and $\{\widehat{\Theta}_{h,j,t}^{TVP-LP,(i)}, j = 1, 2\}_{t=1}^T$, as well as the corresponding accuracy measurements, denoted as $\left\{\widehat{\Omega}_t^{TVP-VAR,(i)}\right\}_{t=1}^T$ and $\left\{\widehat{\Omega}_{h,t}^{TVP-LP,(i)}\right\}_{t=1}^T$. Then we compute the average values of the path estimators across these 2000 replications, denoted as $\{\overline{\widehat{b}}_t^{TVP-VAR}\}_{t=1}^T$, $\{\overline{\widehat{\alpha}}_t^{TVP-VAR}\}_{t=1}^T$, $\{\ln \overline{\widehat{\sigma}}_t^{TVP-VAR}\}_{t=1}^T$, $\{\overline{\widehat{\Theta}}_{h,j,t}^{TVP-VAR}\}_{t=1}^T$, $\{\overline{\widehat{\Theta}}_{h,j,t}^{TVP-LP}\}_{t=1}^T$, $j = 1, 2, h = 2, 3$, as well as the coverage rates across these 2000 Monte Carlo replications, denoted as $\{r_t^{TVP-VAR}\}_{t=1}^T$ and $\{r_{h,t}^{TVP-LP}\}_{t=1}^T$.

Figures 7 and 9 plot the mean path estimates $\{\overline{\widehat{b}}_t^{TVP-VAR}\}_{t=1}^T$, $\{\overline{\widehat{\alpha}}_t^{TVP-VAR}\}_{t=1}^T$, $\{\ln \overline{\widehat{\sigma}}_t^{TVP-VAR}\}_{t=1}^T$,

together with the true parameters of the TVP-VAR in eq.(11), and Figures 8 and 10 plot the mean path estimates $\{\overline{\widehat{\Theta}}^{TVP-VAR}_{h,j,t}\}_{t=1}^{T}$ and $\{\overline{\widehat{\Theta}}^{TVP-LP}_{h,j,t}\}_{t=1}^{T}$, together with the true $\{\Theta_{h,j,t}\}_{t=1}^{T}$ computed using true $\{B_{j,t}\}_{t=1}^{T}$, $j = 1, 2$, $h = 2, 3$, of the TVP-LP in eq.(16), with different specifications. $C = \{0, 5, \cdots, 50\}$ is considered in the estimation procedure.[13] Figures 11 and 12 plot the mean estimates of the TVP-VAR and TVP-LP models, considering different true magnitudes of time variation c for different blocks of parameters ($B_{j,t}$, $\alpha_{ij,t}$, $\ln \sigma_{k,t}$) such that $(c_B, c_\alpha, c_{\ln\sigma}) = (2, 1, 4)$ and different C for different blocks of parameters in the estimation procedure. Results of more model specifications (different T, c, and C for estimation) are provided in the Not-for-Publication Appendix. These figures show that the parameter path estimates perform well with different choices of sample size T, variability parameter c, and the range of C used in the estimation: in fact, all the average path estimates of the TVP-VAR and TVP-LP models are close to the true parameter paths. Smaller values of C give smoother mean path estimates but still recover the trends of the parameter paths; while larger values of C better recover the fluctuations of the parameter paths across time. Besides, the path estimators obtained directly from eq.(16) perform well as the average path estimates of the TVP-LP are close to the true parameter paths. Also, the TVP-LP path estimates perform better than those computed from the TVP-VAR estimates. This might result from the fact that the estimation errors compound while iterating the VAR. In addition, Figures 13-16 plot the coverage rates of intervals constructed using the accuracy measurements of the path estimates for TVP-VAR ($h = 1$) and TVP-LP ($h = 2, 3$) with $T = 240$, $K = 3$, $p = 2$, and $c = 1$ and $C = \{0, 5, \cdots, 50\}$ considered in the estimation procedure. Figures of coverage rates with more specifications (different T, c, and C for estimation) are provided in the Not-for-Publication Appendix. The coverage probabilities generally become more volatile when the magnitude of variability c increases or when T decreases. The WAR minimizing interval estimator generally provides good coverages with different model specifications.

[13] We follow Müller and Petalas (2010) in choosing C.

5 What Are the Macroeconomic Effects of Fiscal Policy Shocks?

Estimates of fiscal policy multipliers differ widely in the literature (see Ramey 2011a). A possible explanation for the wide range of estimates is the fact that the effects of fiscal shocks and the government spending multipliers vary over time. On the one hand, Auerbach and Gorodnichenko (2012), Caggiano, Castelnuovo, Colombo and Nodari (2015), and Fazzari, Morley and Panovska (2015, 2021) find that fiscal multipliers are higher than normal during recessions; on the other hand, Owyang, Ramey and Zubairy (2013) and Ramey and Zubairy (2018) find that the amount of slack in the economy does not substantially affect their size, while the presence of a zero lower bound might. These studies, however, rely on threshold models, which imply a very specific form of time variation that depends on a state variable (e.g., the unemployment rate in Ramey and Zubairy (2018) or capacity utilization in Fazzari, Morley and Panovska (2015)). A similar result, emphasizing that the effects of fiscal policy may depend on the interaction between fiscal and monetary policy has been suggested by Cloyne et al. (2021) and Rossi and Zubairy (2011). More recently, Barnichon, Debortoli and Matthes (2021) find that the multiplier depends on the sign of the shock, i.e., whether the shock is contractionary or expansionary. In this section, we use our proposed methodology to investigate whether the existing literature on the size of fiscal multipliers and the effects of fiscal policy shocks has overlooked potentially important instabilities.

We investigate the effects of fiscal policy shocks using our "agnostic" TVP-LP(-IV) model. Our approach has several advantages relative to state-dependent models: it avoids imposing restrictive assumptions on the type of instability in the data; it uncovers periods in which multipliers are exceptionally high or low; furthermore, it does not take any stand on the source of time variation but rather helps uncovering the economic mechanisms behind it.

5.1 Data and models description

We estimate a quarterly model for the United States including real government spending, real GDP, and a series of government spending shocks over the period 1890:Q1-2015:Q4.[14] The data is transformed as follows. Real government spending is nominal government purchases, including all federal, state, and local purchases but excluding transfer payments, divided by the GDP deflator. The quarterly real government spending is obtained by interpolating annual government spending, combining Kendrick's (1961) annual series starting in 1889 and the annual National Income and Product Accounts (NIPA) data starting in 1929, using monthly federal outlay series from the NBER Macrohistory database and the 1954 quarterly NIPA data from 1939–1946. The quarterly real GDP is obtained by interpolating annual real GDP data, combining the Historical Statistics of the United States series for 1889–1928 and the NIPA data from 1929, using quarterly real GNP series for 1889–1938 and quarterly NIPA nominal GNP data adjusted using the Consumer Price Index (CPI) for 1939–1946. The GDP deflator is constructed using a similar procedure. In addition, all NIPA variables are put in the same units by dividing an estimate of trend GDP, so that one can estimate the multiplier directly.[15]

The fiscal policy shock is identified using a narrative approach based on Ramey (2011b), who measures government spending shocks by estimated changes in the expected present value of government purchases caused by military events; we will refer to them as the "military news shocks".[16]

We use the following TVP-LP to estimate the responses of government spending and GDP to the military news shocks:

$$Y_{i,t+h} = c_t + \theta_{t,h}\epsilon_{f,t} + \psi_t(L)W_t + \xi_{t+h}, \tag{17}$$

where $Y_{i,t}$ is the target variable (either government spending, g_t, or GDP, y_t), the term $\psi_t(L)W_t$ includes control variables, such as lagged values of government spending and GDP, $\epsilon_{f,t}$ is the fiscal

[14] Our choice of sample is guided by Ramey and Zubairy (2018), which is our benchmark for comparisons.
[15] The choice of variables and their transformations closely follow Ramey and Zubairy (2018).
[16] In the Not-for-Publication Appendix, we show that our results are robust to using other identification procedures.

shock, that is Ramey's (2011b) military news shock, and ξ_{t+h} denotes the residuals.

We will compare our results to Ramey and Zubairy's (2018) state-dependent model, where

$$\begin{aligned} Y_{i,t+h} = d_t \left(c_{1,h} + \theta_{1,h}\epsilon_{f,t} + \psi_{1,h}(L)W_t\right) \\ + \left(1 - d_t\right)\left(c_{2,h} + \theta_{2,h}\epsilon_{f,t} + \psi_{2,h}(L)W_t\right) + \xi_{t+h}, \end{aligned} \tag{18}$$

and d_t is a dummy variable such that $d_t = 1$ if a certain state variable (s_t) is above a threshold $\overline{s}$ (i.e, if $s_t > \overline{s}$). Note that eq.(18) is a special case of eq.(17) where $\theta_{t,h} = \theta_{1,h}d_t + \theta_{2,h}\left(1 - d_t\right)$. Compared with the state-dependent model in eq.(18), the TVP-LP in eq.(17) allows the parameters to vary in a flexible way over time, rather than allowing only changes across states. Furthermore, it allows us to study whether a state-dependent model sufficiently describes all the heterogeneity of the responses over time.

Another special case is the constant parameter model, where $\theta_{t,h} = \theta_h$, that is:

$$Y_{i,t+h} = c_h + \theta_h\epsilon_{f,t} + \psi_h(L)W_t + \xi_{t+h}. \tag{19}$$

The fiscal multipliers are calculated as the ratio of the integral of the output responses and the integral of the government spending responses, and measure the cumulative GDP gains relative to the cumulative government spending over the period. In the TVP-LP-IV model, the multipliers $(m_{t,h})$ are obtained as follows: $\sum_{j=0}^{h} y_{t+j} = \mu_{y,t,h} + m_{t,h}\sum_{j=0}^{h} g_{t+j} + \phi_{y,t,h}(L)W_t + v_{y,t+h}$, where y_t and g_t refer to GDP and government spending respectively, via an instrumental variable approach using $\epsilon_{f,t}$ as an instrument for $\sum_{j=0}^{h} g_{t+j}$. In practice, they are estimated using the following equation:

$$\begin{bmatrix} \sum_{j=0}^{h} g_{t+j} \\ \sum_{j=0}^{h} y_{t+j} \end{bmatrix} = \mu_{t,h} + \begin{bmatrix} \pi_{t,h} \\ \pi_{t,h}m_{t,h} \end{bmatrix} \epsilon_{f,t} + \Phi_{t,h}(L)W_t + v_{t+h}. \tag{20}$$

We assume v_{t+h} is normally distributed with mean zero and covariance matrix $\Sigma_{v,t+h}$, and get the likelihood accordingly.

We will compare our multipliers to Ramey and Zubairy's (2018) state-dependent model, where

$$\begin{bmatrix} \sum_{j=0}^{h} g_{t+j} \\ \sum_{j=0}^{h} y_{t+j} \end{bmatrix} = d_t \left(\mu_{1,h} + \begin{bmatrix} \pi_{1,h} \\ \pi_{1,h} m_{1,h} \end{bmatrix} \epsilon_{f,t} + \phi_{1,h}(L) W_t \right) + (1 - d_t) \left(\mu_{2,h} + \begin{bmatrix} \pi_{2,h} \\ \pi_{2,h} m_{2,h} \end{bmatrix} \epsilon_{f,t} + \Phi_{2,h}(L) W_t \right) + v_{t+h}, \tag{21}$$

which is a special case of our eq.(20) where $\pi_{t,h} m_{t,h} = d_t \pi_{1,h} m_{1,h} + (1 - d_t)\, \pi_{2,h} m_{2,h}$. Another special case is the constant parameter model, where $m_{t,h} = m_h$, that is:

$$\begin{bmatrix} \sum_{j=0}^{h} g_{t+j} \\ \sum_{j=0}^{h} y_{t+j} \end{bmatrix} = \mu_h + \begin{bmatrix} \pi_h \\ \pi_h m_h \end{bmatrix} \epsilon_{f,t} + \Phi_h(L) W_t + v_{t+h}. \tag{22}$$

5.2 Understanding time variation in the effects of fiscal policy shocks and government spending multipliers

First, we test for the existence of parameter instabilities. We implement Elliott and Müller's (2006) qLL test in the government spending and GDP equations in eq.(17), with $h = 1$. The test finds significant evidence of instabilities. In fact, the qLL test statistics are -105.57 and -120.61 respectively, and are smaller than the critical value at the 1% significance level. Besides, if we focus on the state-dependent model in eq.(18) with $h = 1$, the qLL test statistics for the government spending and GDP equations are -144.46 and -153.77 respectively when the state variable is unemployment and -125.45 and -135.27 respectively the state variable is the ZLB. All are smaller than the critical value at the 1% significance level. This suggests the presence of instabilities even in the state-dependent model.

Next, we turn to the responses to fiscal policy shocks.[17] Figures 17-18 plot impulse responses of government spending and GDP to Ramey and Zubairy's (2018) military news shock from three

[17] In our estimates, we consider vector c_i with $C = \{0, 3, \cdots, 15\}$ for the intercepts and slope parameters and $C = \{0, 3, \cdots, 15\}$ for the variance parameters.

models: (i) the linear model, eq.(19); (ii) Ramey and Zubairy's (2018) state-dependent models, eq.(18), characterizing the state by either the unemployment level or whether the ZLB holds; (iii) our TVP-LP which, instead, allows the parameters to vary across all time periods. In the figure, we sort our time-varying responses (which differ at each point in time) in two groups, identified based on how the date is classified depending on the value of the state variables. As shown in Figures 17-18, the TVP-LP responses are heterogeneous across time: they vary a lot depending on the period and not only on the value of the state, thus containing richer information than state-dependent models. The Not-for-Publication Appendix reports robustness results to fiscal shocks identified in alternative ways as well as results including more control variables.

We then calculate the cumulative spending multipliers ($m_{t,h}$ in eq.(20)) for two- and four-year-ahead horizons using the news shocks as an instrument. The results are reported in Table 1. The table reports fiscal multipliers from linear and state-dependent models considering the clarifications "recession/expansion"[18] and "ZLB/Normal periods", as well as our TVP-LP-IV results for selected dates (1938:Q1, 1945:Q1, 1954:Q1, 1984:Q1). These dates are chosen such that they belong to different states: in particular, 1938:Q1, 1945:Q1, 1945:Q1, 1984:Q1 are classified as "Recession, Expansion, Expansion, Recession", and "ZLB, ZLB, Normal, Normal". As shown in Table 1, Ramey and Zubairy's (2018) state-dependent results imply that the multiplier is larger in recession/ZLB periods than that in expansion/Normal periods. However, our TVP-LP-IV multipliers behave differently depending on the date. In particular, our TVP-LP-IV multipliers in recessions (1938:Q1, 1984:Q1) are smaller than those in expansions (1945:Q1, 1954:Q1). Most interestingly, the pattern of our TVP-LP-IV multipliers in the chosen periods do not correspond to ZLB/Normal periods either.

Thus, the table suggests that our TVP-LP-IV multipliers vary depending on the date, with different patterns from those based on the state-dependent model, no matter whether the state is high/low unemployment or the presence of the zero lower bound.

To investigate more systematically whether our time-varying multipliers can be fully character-

[18] Ramey and Zubairy (2018) define an economy to be in a slack state when the unemployment rate is above 6.5.

ized by a state-dependent model, consider Figures 19 - 20. Figure 19 plots our multipliers together with shaded areas indicating times when unemployment is above the threshold. Clearly, the time variation cannot be fully explained by recessionary/expansionary periods. Figure 20 instead plots our multipliers together with shaded areas indicating whether the economy is at the zero lower bound: the time variation cannot be fully explained by the presence of the zero lower bound either. Our TVP-LP-IV multipliers are significantly different from the state-dependent multipliers in some periods – for example, see periods around 1950 in Figures 19(a) and 20(a).

Figure 21 further shows our cumulative spending multipliers for several horizons during "recessions"(panels on the top left), "expansions"(panels on the top right), as well as "ZLB"(panels on the bottom left), and "non-ZLB"(panels on the bottom right) periods, together with Ramey and Zubairy's (2018) multipliers, respectively. For example, the top left panel in Figure 21 plots the multipliers based on: (i) the linear model (line with circles); (ii) periods labeled "recessions"according to Ramey and Zubairy's (2018) state-dependent model (dashed line); and (iii) our TVP-LP-IV path estimators (continuous line) in all periods that are classified as recessionary – i.e., the unemployment rates are higher than 6.5%. Figure 21 implies that the cumulative multipliers differ from those in Ramey and Zubairy's (2018) linear and state-dependent models and exhibit strong variation across time. Thus, our approach captures information that might be lost when considering constant parameters in a given state. Besides, the TVP-LP-IV multipliers in periods classified as recessionary are very different from those obtained from Ramey and Zubairy's (2018) state-dependent model, implying that unemployment rates may not be the only/correct factor that describes the variation across multipliers.

In addition, Figure 22 plots the TVP-LP-IV cumulative spending multipliers at the beginning of several wars: the Spanish-American War, starting with the sinking of the USS Maine (1898:Q1), the start of WW-I (1914:Q3) and WW-II (1939:Q3), the start of the Korean (1950:Q3) and Vietnam (1965:Q1) wars, the fiscal buildup in response to the Soviet invasion of Afghanistan (1980:Q1), and the terrorist attack on 9/11 (2001:Q3). Our TVP-LP-IV multipliers differ across each war date. For example, consider Figure 22(d), which shows that our TVP-LP-IV multipliers at the start

of the Korean (1950:Q3) substantially differ from both the linear and state-dependent models' multipliers.

In a recent paper, Barnichon, Debortoli and Matthes (2021) argue that the fiscal multiplier is low (below unity) for expansionary shocks (that is, shocks that increase government spending) and large (above unity) for contractionary shocks. They conclude that, since narrative shocks typically contain larger and more frequently positive shocks than negative ones, the multipliers are typically below unity and display no detectable state-dependence. Figure 24(a) plots our estimated multipliers $m_{t,h}$ in eq.(20) together with the fiscal policy shocks. As in Barnichon, Debortoli and Matthes (2021), we notice that the multiplier starts to increase substantially in the presence of positive shocks. However, that is not always the case; for example, in 1950Q2, there is a large positive shock yet the multiplier starts decreasing from that point onwards. Similarly, there are large increases in the 4-year multiplier around 1920 yet no large positive shocks to explain that increase. So, while our results generally support Barnichon, Debortoli and Matthes's (2021) intuition, the sign of the shock does not completely explain the fluctuations of the multipliers over time.

By looking more closely to the time variation in the multipliers and their correlation with other potential explanatory variables, we can shed light on whether alternative variables can be more successful in explaining why fiscal multipliers change over time. In particular, our analysis suggests that the multiplier is correlated with U.S. public debt. In fact, Figure 24(b) plots our estimated multipliers m_t in eq.(20) together with public debt. It is clear that the multipliers comove with public debt. Hence, not only the sign of fiscal policy shocks is important, but also the size of public debt. Let us investigate whether a state dependent model where the state is public debt explains the multipliers' evolution over time better than the traditional state variables previously considered in the literature. Figure 25 plots 1/4-year integral multipliers based on our TVP-LP-IV as well as the state dependent model where the state variable is public debt.[19] By comparing Figure 25 with Figures 19-20, it is clear that using public debt as the state variable

[19]The historical public debt is documented annually and we use the detrended public debt from the previous year as the state variable. We consider a threshold value of 11. Other choices of threshold values give robust results.

describes the time variation better than using unemployment or the interest rate. This analysis further demonstrates the usefulness of our TVP-LP(-IV) methodology as a flexible framework to model time variation and investigate the reasons behind it.

6 Conclusion

This paper introduces time variation in the local projections framework, allowing local instabilities in both slope coefficients and variances, and develops an estimator for impulse responses in unstable local projections. Monte Carlo studies demonstrate the good performance of both the TVP-VAR and TVP-LP path estimators in finite samples. Our methodology uncovers novel results on fiscal multipliers. Our estimated responses of government spending and GDP to fiscal policy shocks as well as the cumulative spending multipliers are heterogeneous across time: their evolution over time cannot be adequately characterized by traditional state variables, such as unemployment or whether the economy is at the zero lower bound, thus featuring richer information than state-dependent models. We also find that the sign of the fiscal policy shock does not completely explain the fluctuations of the multipliers either; the size of public debt, instead, emerges as an important explanatory variables.

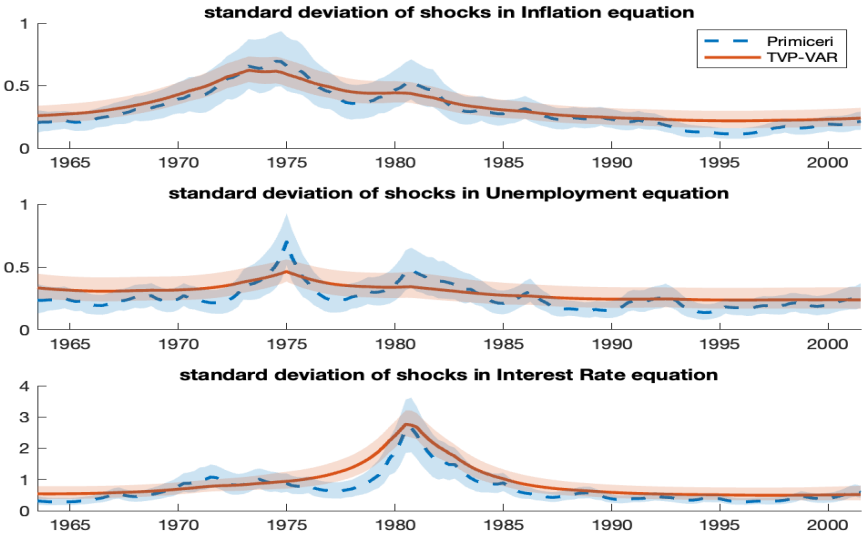

Figure 1: Standard deviation of the shocks in each equation

Note: This figure plots the standard deviation of the shocks of (a) the inflation equation, (b) the unemployment equation, and (c) the interest rate equation (monetary policy shocks), based on Primiceri's (2005) TVP-BVAR and our TVP-VAR estimates, respectively. The blue and red areas are the 90% confidence bands.

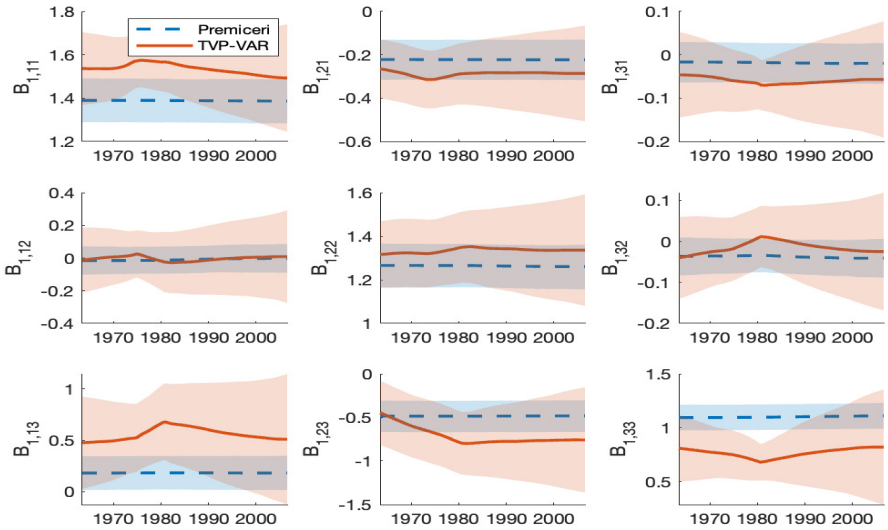

Figure 2: TVP-VAR Path estimates of $B_{1,t}$

Note: This figure plots the path estimates of the parameter matrix $B_{1,t}$, based on Primiceri's (2005) TVP-BVAR and our TVP-VAR estimates, respectively. $B_{1,rs}$ refers to the r^{th} row and s^{th} column element in the parameter matrix $B_{1,t}$. The blue and red areas are the 90% confidence bands.

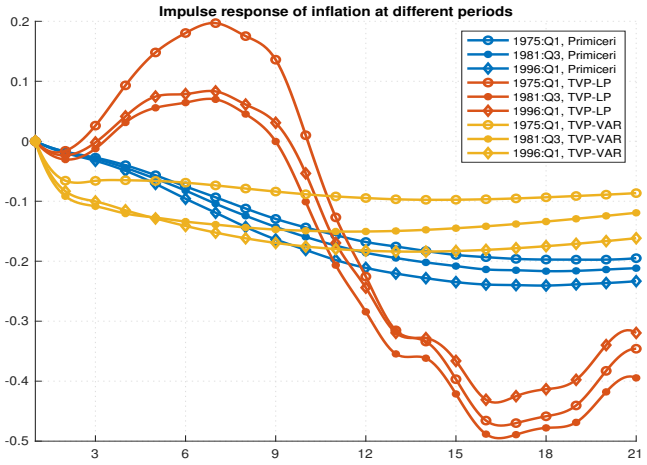

(a) inflation

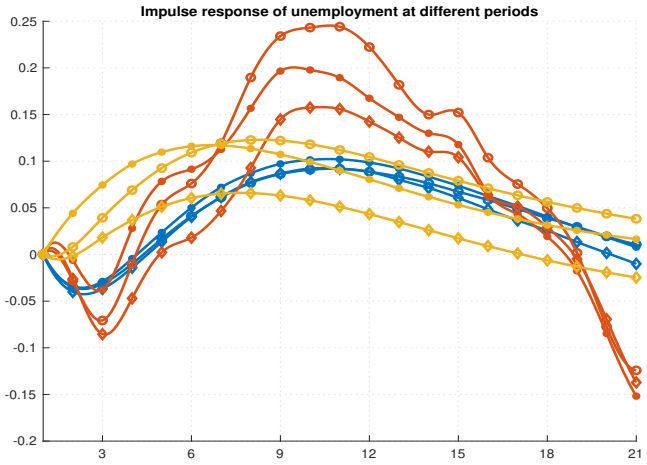

(b) unemployment

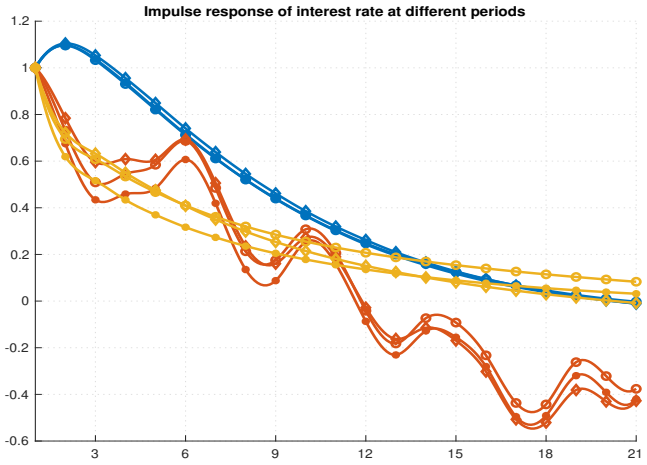

(c) interest rate

Figure 3: Impulse responses of each variable to a unit monetary policy shock at different periods

Note: This figure plots the impulse responses of each variable to a unit monetary policy shock at various periods (1975:Q1, 1981:Q3, 1996:Q1), based on Primiceri's (2005) TVP-BVAR estimates (in blue), our TVP-LP estimates (in red), and our TVP-VAR estimates (in orange), respectively. The x-axis refers to horizons (quarters).

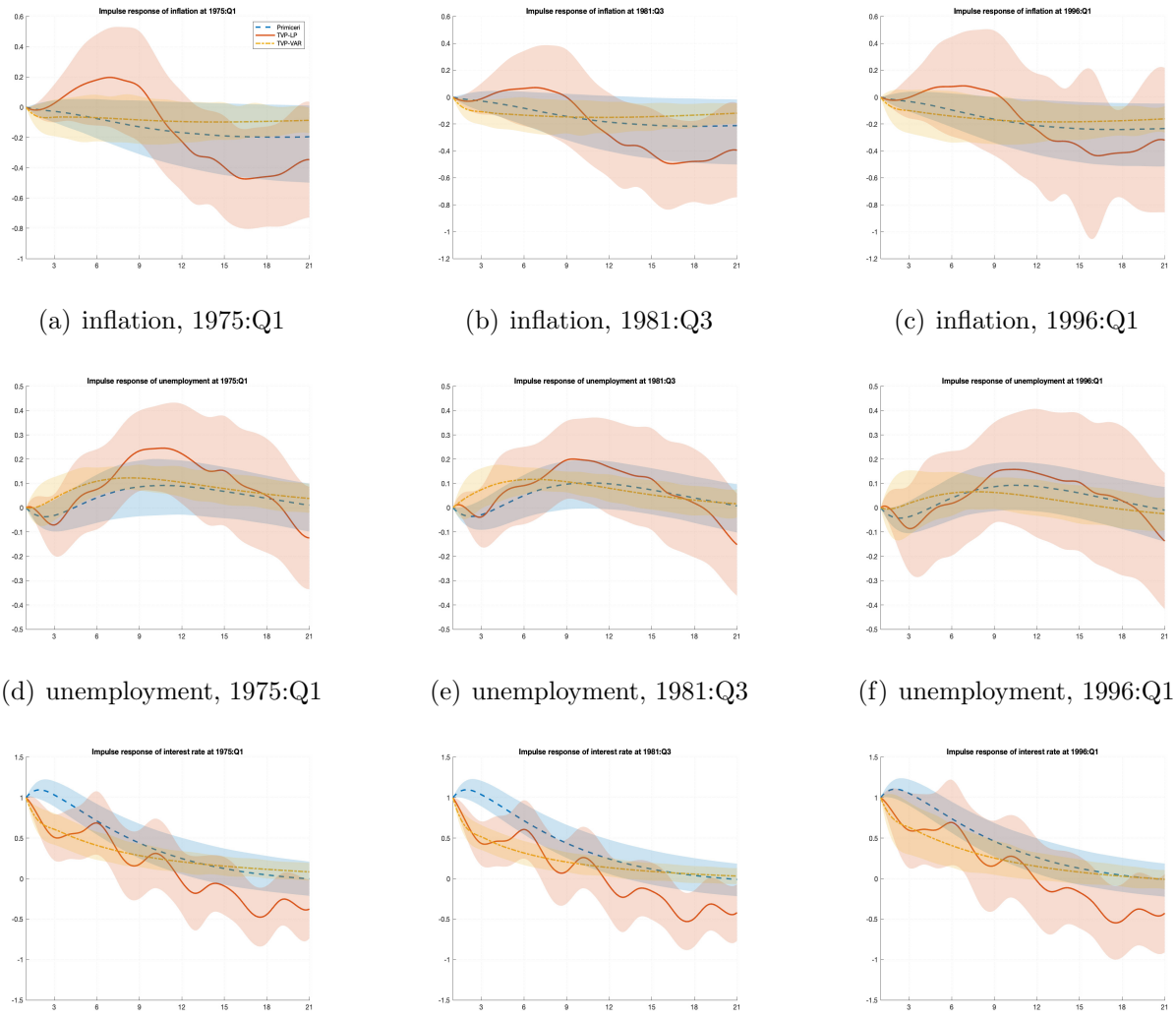

(a) inflation, 1975:Q1 (b) inflation, 1981:Q3 (c) inflation, 1996:Q1

(d) unemployment, 1975:Q1 (e) unemployment, 1981:Q3 (f) unemployment, 1996:Q1

(g) interest rate, 1975:Q1 (h) interest rate, 1981:Q3 (i) interest rate, 1996:Q1

Figure 4: Impulse responses of each variable to a unit monetary policy shock at different periods

Note: This figure plots the impulse responses of each variable to a unit monetary policy shock at each period (1975:Q1, 1981:Q3, 1996:Q1), based on Primiceri's (2005) TVP-BVAR estimates (in blue), our TVP-LP estimates (in red), and our TVP-VAR estimates (in orange), respectively. The shaded areas are the 90% confidence bands. The x-axis refers to horizons (quarters).

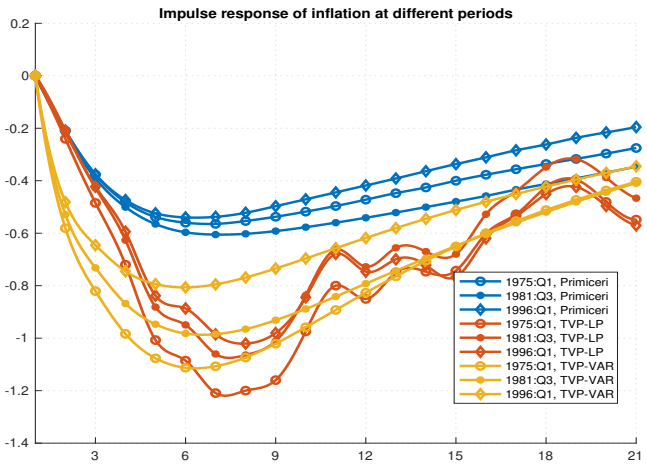

(a) inflation

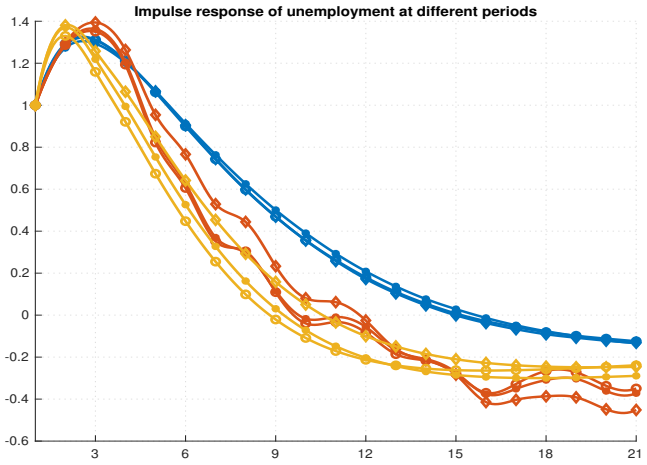

(b) unemployment

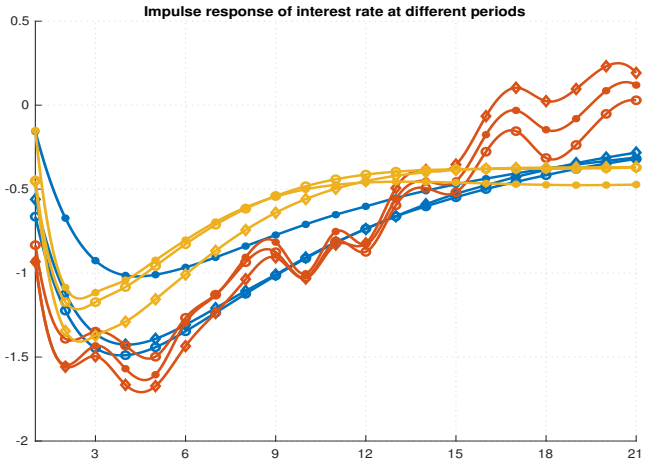

(c) interest rate

Figure 5: Impulse responses of each variable to a unit unemployment shock at different periods

Note: This figure plots the impulse responses of each variable to a 1% permanent increase in unemployment at various periods (1975:Q1, 1981:Q3, 1996:Q1), based on Primiceri's (2005) TVP-BVAR estimates (in blue), our TVP-LP estimates (in red), and our TVP-VAR estimates (in orange), respectively. The x-axis refers to horizons (quarters).

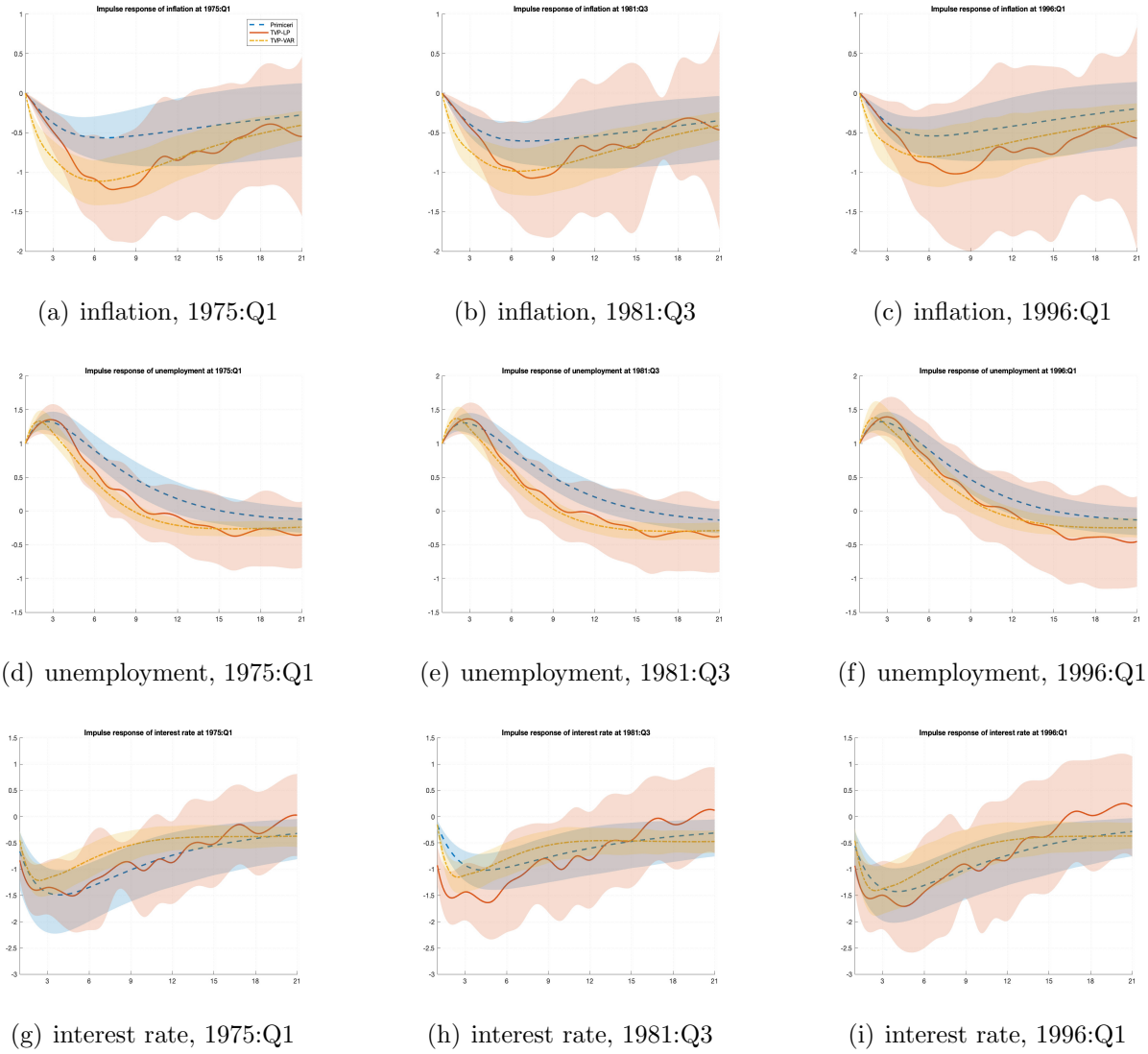

(a) inflation, 1975:Q1 (b) inflation, 1981:Q3 (c) inflation, 1996:Q1

(d) unemployment, 1975:Q1 (e) unemployment, 1981:Q3 (f) unemployment, 1996:Q1

(g) interest rate, 1975:Q1 (h) interest rate, 1981:Q3 (i) interest rate, 1996:Q1

Figure 6: Impulse responses of each variable to a unit unemployment shock at different periods

Note: This figure plots the impulse responses of each variable to a 1% permanent increase in unemployment at each period (1975:Q1, 1981:Q3, 1996:Q1), based on Primiceri's (2005) TVP-BVAR estimates (in blue), our TVP-LP estimates (in red), and our TVP-VAR estimates (in orange), respectively. The shaded areas are the 90% confidence bands. The x-axis refers to horizons (quarters).

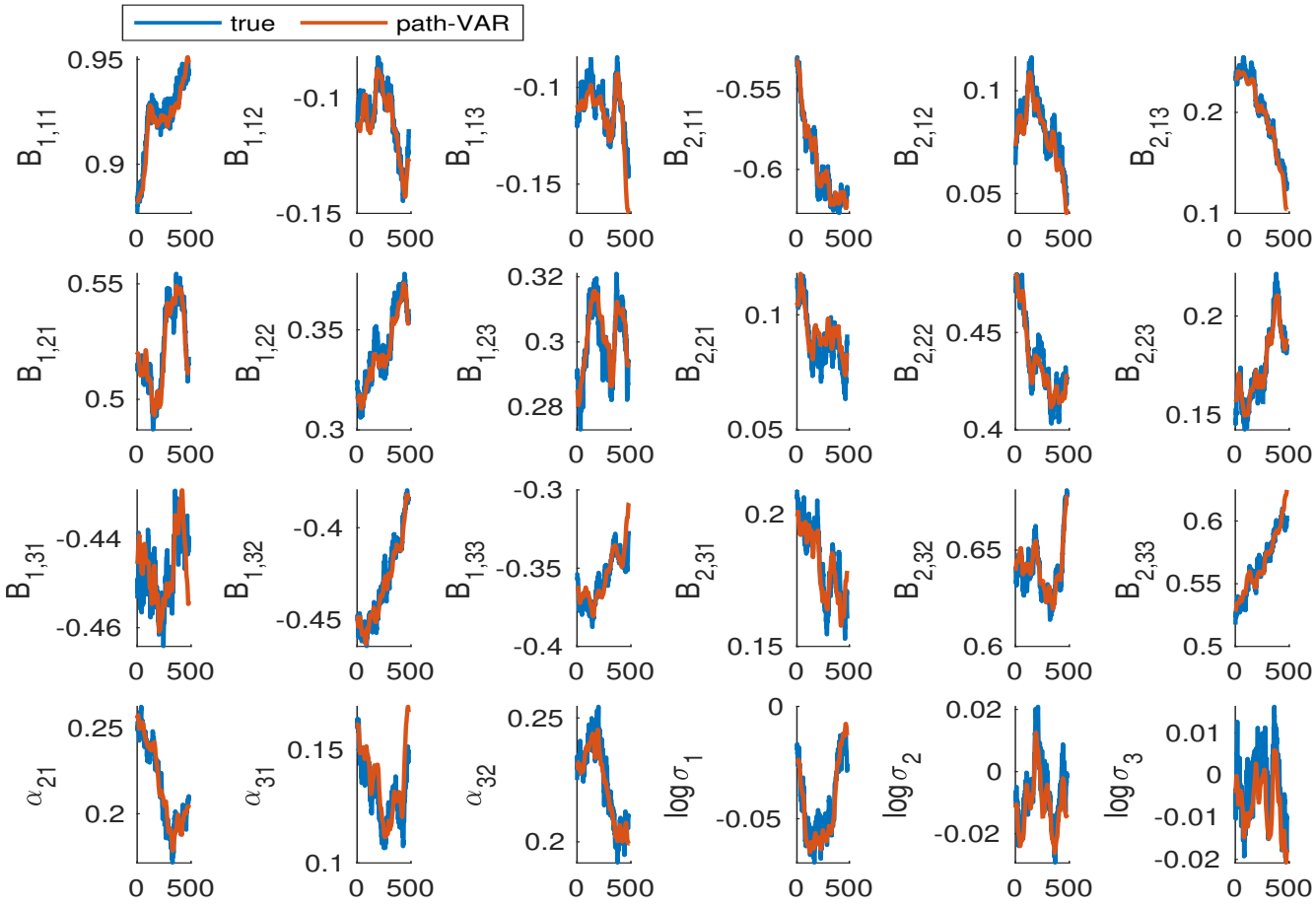

Figure 7: TVP-VAR path estimates, $T = 480$, $K = 3$, $p = 2$, $c = 1$, $C = \{0, 5, \cdots, 50\}$

Note: This figure plots the average values of the TVP-VAR path estimates with $T = 480$, $K = 3$, $p = 2$, $c = 1$ across 2000 replications. $C = \{0, 5, \cdots, 50\}$ is considered in the estimation procedure. The blue lines are the true parameter values of $\{B_{j,t}\}_{t=1}^{T}, j = 1, 2$, $\{\alpha_{ij,t}\}_{t=1}^{T}, i = 2, \cdots, K, j < i$, $\{\ln \sigma_{k,t}\}_{t=1}^{T}, k = 1, \cdots, K$, and the red lines are the average path estimates $\{\overline{\widehat{B}}_{j,t}^{TVP-VAR}\}_{t=1}^{T}, j = 1, 2$, $\{\overline{\widehat{\alpha}}_{ij,t}^{TVP-VAR}\}_{t=1}^{T}, i = 2, \cdots, K, j < i$, $\{\ln \overline{\widehat{\sigma}}_{k,t}^{TVP-VAR}\}_{t=1}^{T}, k = 1, \cdots, K$. The x-axis refers to the periods, and y-axis refers to the parameters. The notation $B_{j,rs}, j = 1, 2$ refers to the r^{th} row and s^{th} column element in the parameter matrix $B_{j,t}, j = 1, 2$.

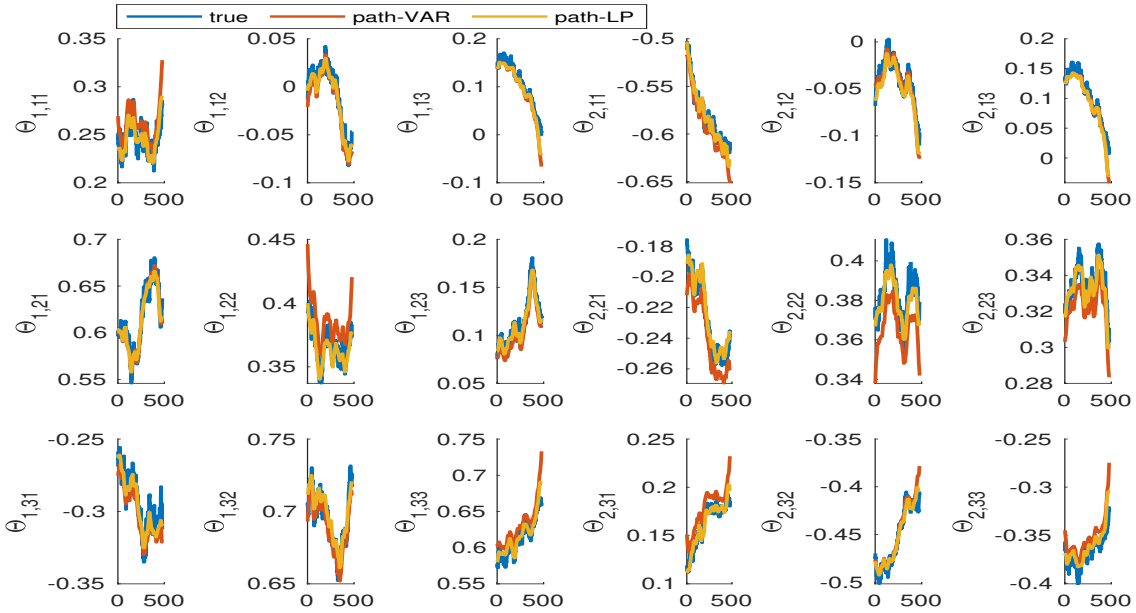

(a) $h = 2$

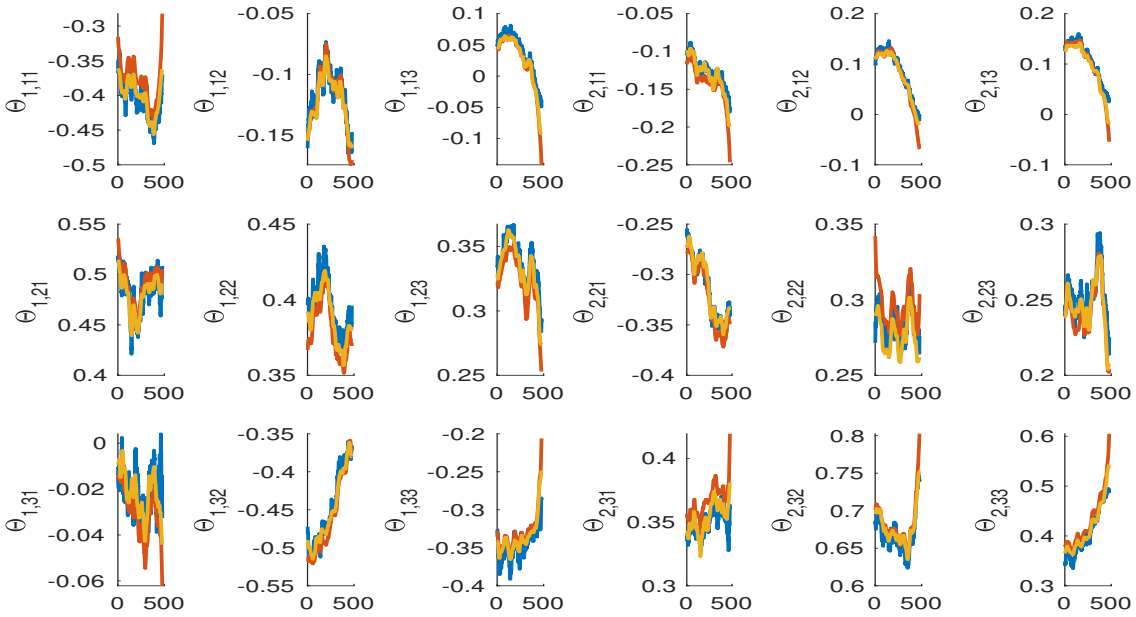

(b) $h = 3$

Figure 8: TVP-LP path estimates, $T = 480$, $K = 3$, $p = 2$, $c = 1$

Note: This figure plots the average values of the TVP-LP path estimates with $T = 480$, $K = 3$, $p = 2$, $c = 1$ across 2000 replications, and different C is considered in the estimation procedure. The blue lines are the true parameter values of $\{\Theta_{h,j,t}\}_{t=1}^{T}$, the red and orange lines are the average path estimates $\{\overline{\widehat{\Theta}}_{h,j,t}^{TVP-VAR}\}_{t=1}^{T}$ and $\{\overline{\widehat{\Theta}}_{h,j,t}^{TVP-LP}\}_{t=1}^{T}$, respectively. The x-axis refers to the periods, and y-axis refers to the parameters where the subscripts h and t are omitted for notational simplicity. The notation $\Theta_{j,rs}$ refers to the r^{th} row and s^{th} column element in the parameter matrix $\Theta_{h,j,t}$ with different h in (a) and (b).

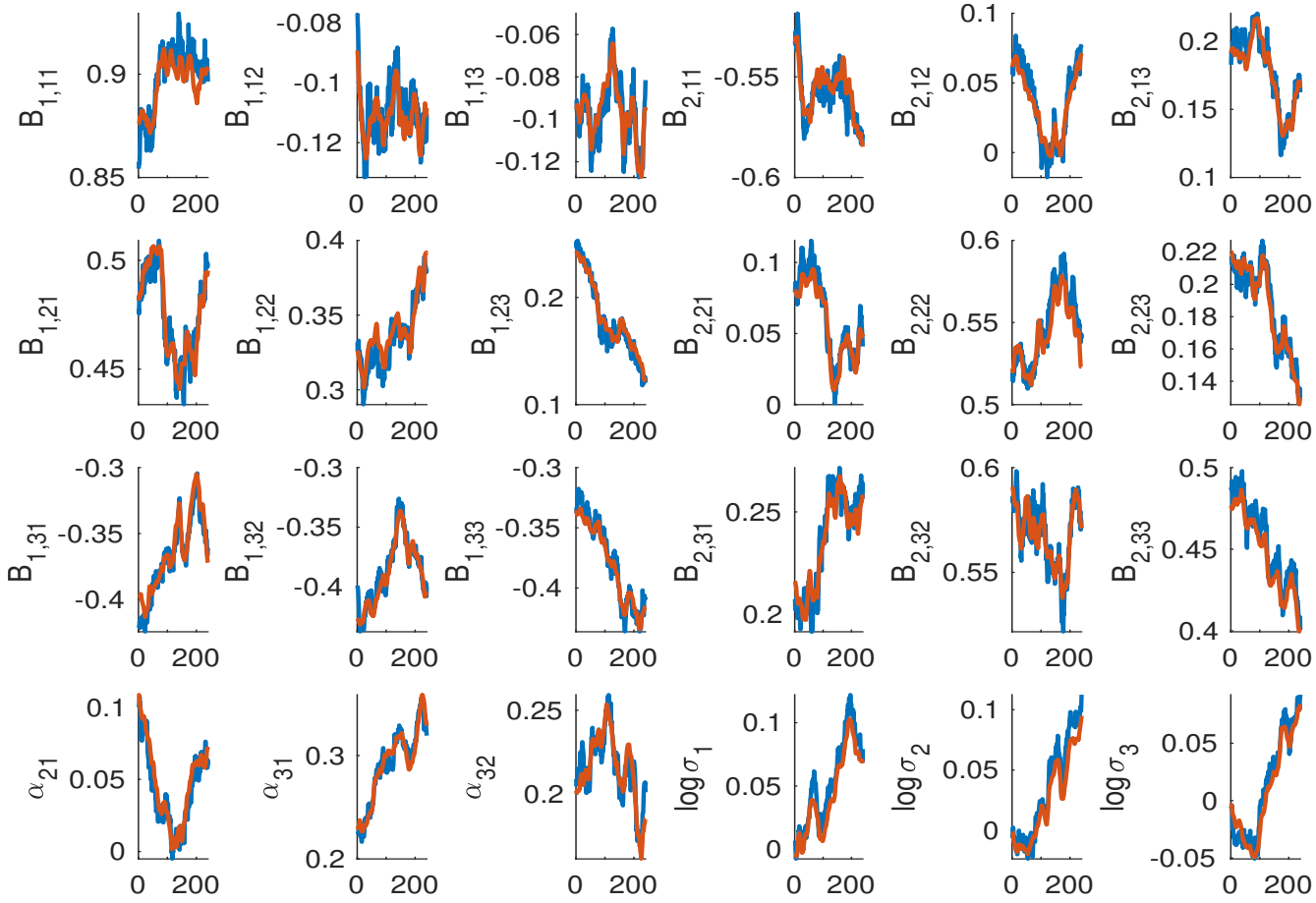

Figure 9: TVP-VAR path estimates, $T = 240$, $K = 3$, $p = 2$, $c = 1$, $C = \{0, 5, \cdots, 50\}$

Note: This figure plots the average values of the TVP-VAR path estimates with $T = 240$, $K = 3$, $p = 2$, $c = 1$ across 2000 replications. $C = \{0, 5, \cdots, 50\}$ is considered in the estimation procedure. The blue lines are the true parameter values of $\{B_{j,t}\}_{t=1}^{T}, j = 1, 2$, $\{\alpha_{ij,t}\}_{t=1}^{T}, i = 2, \cdots, K, j < i$, $\{\ln \sigma_{k,t}\}_{t=1}^{T}, k = 1, \cdots, K$, and the red lines are the average path estimates $\{\overline{\widehat{B}}_{j,t}^{TVP-VAR}\}_{t=1}^{T}, j = 1, 2$, $\{\overline{\widehat{\alpha}}_{ij,t}^{TVP-VAR}\}_{t=1}^{T}, i = 2, \cdots, K, j < i$, $\{\ln \overline{\widehat{\sigma}}_{k,t}^{TVP-VAR}\}_{t=1}^{T}, k = 1, \cdots, K$. The x-axis refers to the periods, and y-axis refers to the parameters. The notation $B_{j,rs}, j = 1, 2$ refers to the r^{th} row and s^{th} column element in the parameter matrix $B_{j,t}, j = 1, 2$.

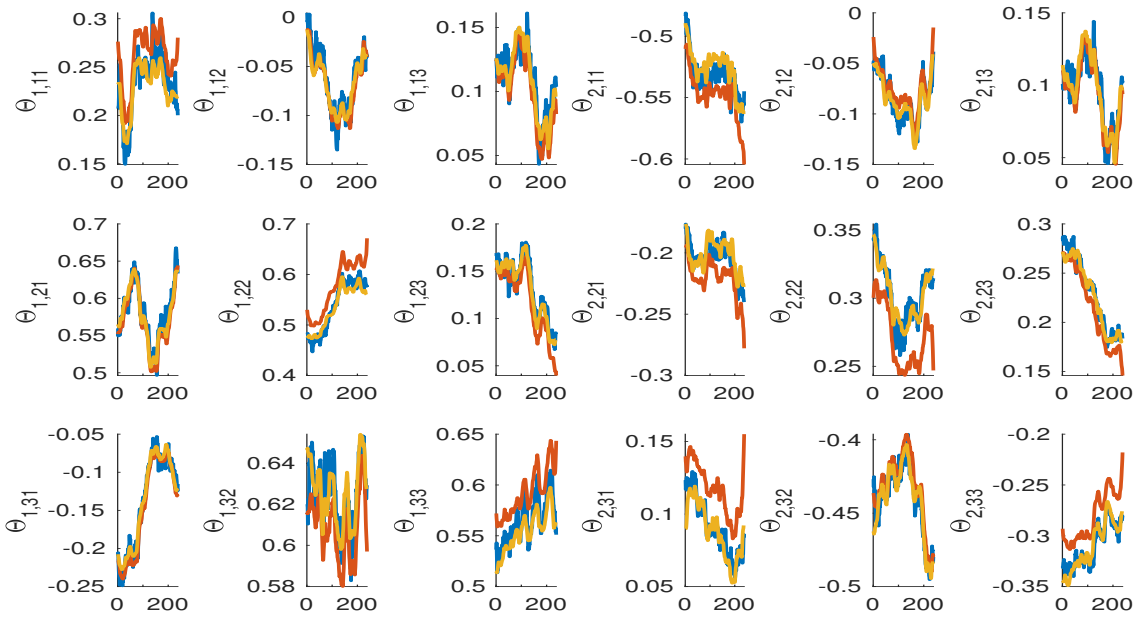

(a) $h = 2$

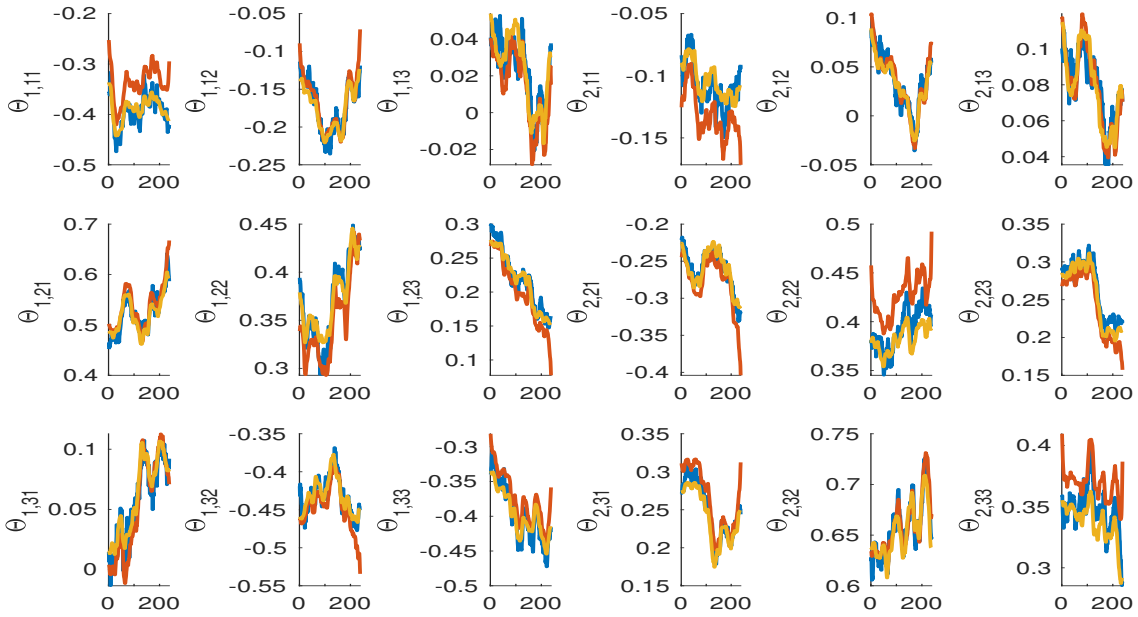

(b) $h = 3$

Figure 10: TVP-LP path estimates, $T = 240$, $K = 3$, $p = 2$, $c = 1$

Note: This figure plots the average values of the TVP-LP path estimates with $T = 240$, $K = 3$, $p = 2$, $c = 1$ across 2000 replications, and different C is considered in the estimation procedure. The blue lines are the true parameter values of $\{\Theta_{h,j,t}\}_{t=1}^{T}$, the red and orange lines are the average path estimates $\{\overline{\widehat{\Theta}}_{h,j,t}^{TVP-VAR}\}_{t=1}^{T}$ and $\{\overline{\widehat{\Theta}}_{h,j,t}^{TVP-LP}\}_{t=1}^{T}$, respectively. The x-axis refers to the periods, and y-axis refers to the parameters where the subscripts h and t are omitted for notational simplicity. The notation $\Theta_{j,rs}$ refers to the r^{th} row and s^{th} column element in the parameter matrix $\Theta_{h,j,t}$ with different h in (a) and (b).

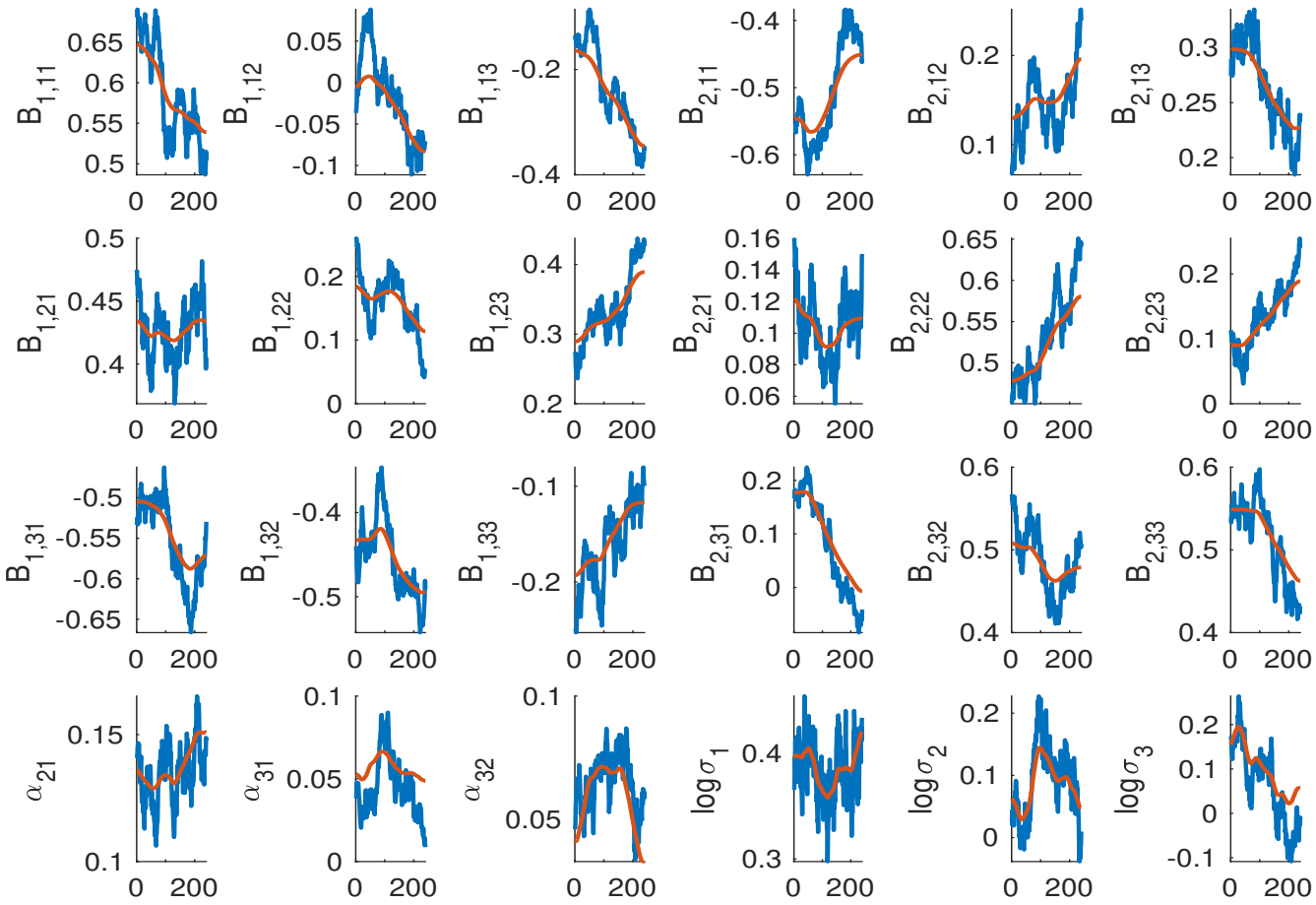

Figure 11: TVP-VAR path estimates, $T = 240$, $K = 3$, $p = 2$, $(c_B, c_\alpha, c_{\ln\sigma}) = (2, 1, 4)$, $C_B = \{0, 2, \cdots, 6\}$, $C_\alpha = \{0, 3, \cdots, 9\}$, $C_{\ln\sigma} = \{0, 3, \cdots, 15\}$

Note: This figure plots the average values of the TVP-VAR path estimates with $T = 240$, $K = 3$, $p = 2$ across 2000 replications. The true magnitudes of time variation c are different for different blocks of parameters ($B_{j,t}$, $\alpha_{ij,t}$, $\ln\sigma_{k,t}$) such that $(c_B, c_\alpha, c_{\ln\sigma}) = (2, 1, 4)$. Different ranges of C ($C_B = \{0, 2, \cdots, 6\}$, $C_\alpha = \{0, 3, \cdots, 9\}$, $C_{\ln\sigma} = \{0, 3, \cdots, 15\}$) are considered for different blocks of parameters are considered in the estimation procedure. The blue lines are the true parameter values of $\{B_{j,t}\}_{t=1}^{T}, j = 1, 2$, $\{\alpha_{ij,t}\}_{t=1}^{T}, i = 2, \cdots, K, j < i$, $\{\ln\sigma_{k,t}\}_{t=1}^{T}, k = 1, \cdots, K$, and the red lines are the average path estimates $\{\overline{\widehat{B}}_{j,t}^{TVP-VAR}\}_{t=1}^{T}, j = 1, 2$, $\{\overline{\widehat{\alpha}}_{ij,t}^{TVP-VAR}\}_{t=1}^{T}, i = 2, \cdots, K, j < i$, $\{\ln\overline{\widehat{\sigma}}_{k,t}^{TVP-VAR}\}_{t=1}^{T}, k = 1, \cdots, K$. The x-axis refers to the periods, and y-axis refers to the parameters. The notation $B_{j,rs}, j = 1, 2$ refers to the r^{th} row and s^{th} column element in the parameter matrix $B_{j,t}, j = 1, 2$.

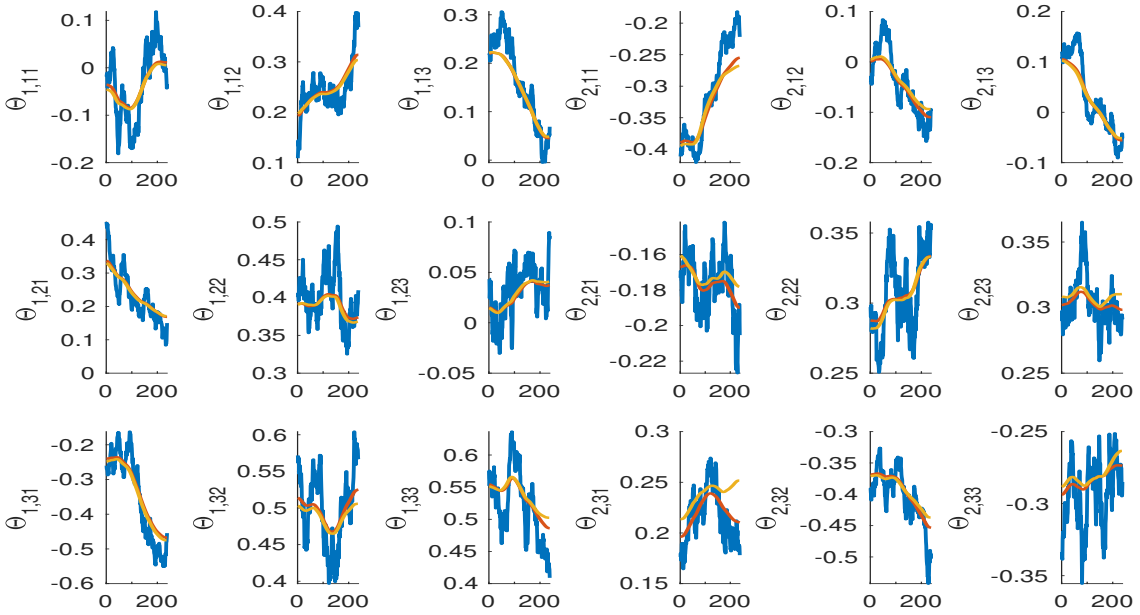

(a) $h = 2$

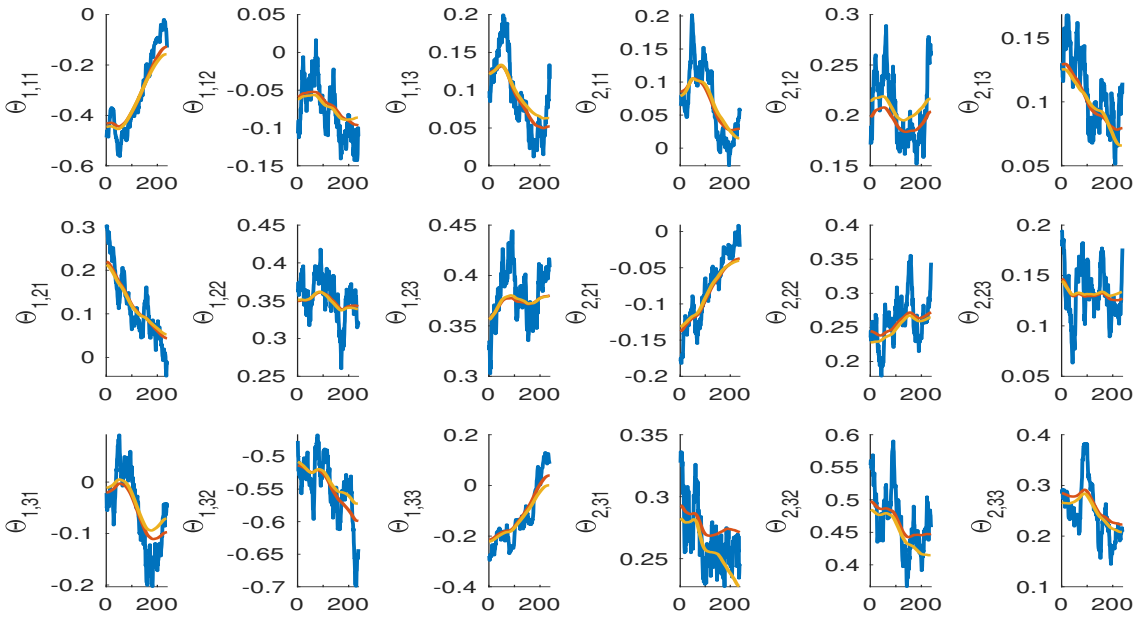

(b) $h = 3$

Figure 12: TVP-LP path estimates, $T = 240$, $K = 3$, $p = 2$, $(c_B, c_\alpha, c_{\ln\sigma}) = (2, 1, 4)$, $C_B = \{0, 2, \cdots, 6\}$, $C_\alpha = \{0, 3, \cdots, 9\}$, $C_{\ln\sigma} = \{0, 3, \cdots, 15\}$

Note: This figure plots the average values of the TVP-LP path estimates with $T = 240$, $K = 3$, $p = 2$ across 2000 replications. The true magnitudes of time variation c are different for different blocks of parameters ($B_{j,t}$, $\alpha_{ij,t}$, $\ln\sigma_{k,t}$) such that $(c_B, c_\alpha, c_{\ln\sigma}) = (2, 1, 4)$. Different ranges of C ($C_B = \{0, 2, \cdots, 6\}$, $C_\alpha = \{0, 3, \cdots, 9\}$, $C_{\ln\sigma} = \{0, 3, \cdots, 15\}$) are considered for different blocks of parameters are considered in the estimation procedure. The blue lines are the true parameter values of $\{\Theta_{h,j,t}\}_{t=1}^{T}$, the red and orange lines are the average path estimates $\{\overline{\widehat{\Theta}}_{h,j,t}^{TVP-VAR}\}_{t=1}^{T}$ and $\{\overline{\widehat{\Theta}}_{h,j,t}^{TVP-LP}\}_{t=1}^{T}$, respectively. The x-axis refers to the periods, and y-axis refers to the parameters where the subscripts h and t are omitted for notational simplicity. The notation $\Theta_{j,rs}$ refers to the r^{th} row and s^{th} column element in the parameter matrix $\Theta_{h,j,t}$ with different h in (a) and (b).

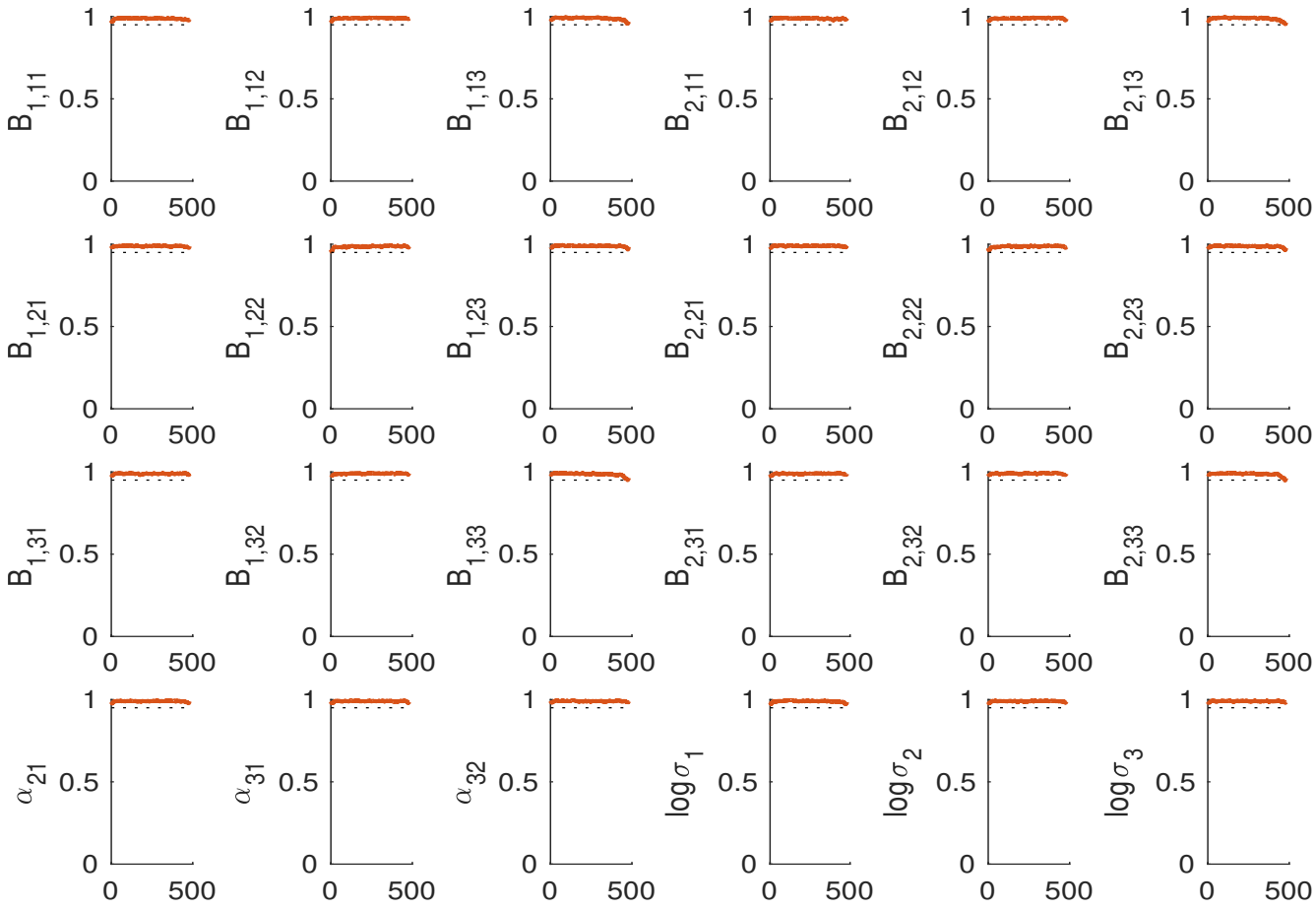

Figure 13: Coverage rates of TVP-VAR credible intervals, $T = 480$, $K = 3$, $p = 2$, $c = 1$, $C = \{0, 5, \cdots, 50\}$

Note: This figure plots the coverage rates of TVP-VAR credible intervals with $T = 480$, $K = 3$, $p = 2$, $c = 1$ across 2000 replications. $C = \{0, 5, \cdots, 50\}$ is considered in the estimation procedure. The black dotted line is the 95% horizontal line. The notation $B_{j,rs}, j = 1, 2$ refers to the r^{th} row and s^{th} column element in the parameter matrix $B_{j,t}, j = 1, 2$.

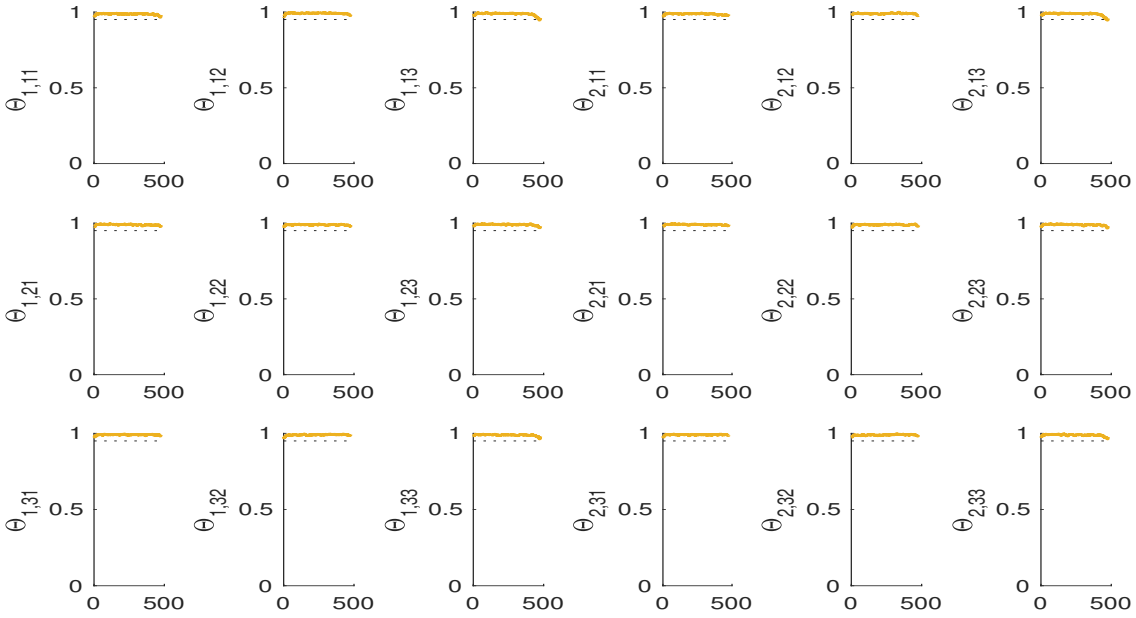

(a) $h = 2$

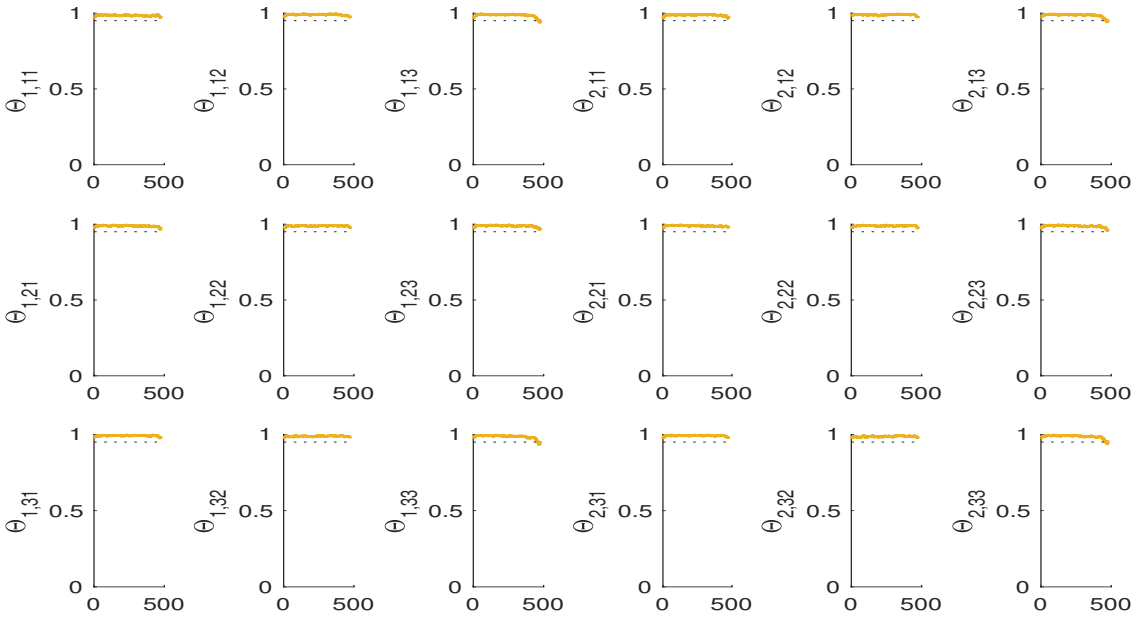

(b) $h = 3$

Figure 14: Coverage rates of TVP-LP credible intervals, $T = 480$, $K = 3$, $p = 2$, $c = 1$, $C = \{0, 5, \cdots, 50\}$

Note: This figure plots the coverage rates of TVP-LP credible intervals with $T = 240$, $K = 3$, $p = 2$, $c = 1$ across 2000 replications. $C = \{0, 5, \cdots, 50\}$ is considered in the estimation procedure. The black dotted line is the 95% horizontal line. The x-axis refers to the periods, and y-axis refers to the parameters where the subscripts h and t are omitted for notational simplicity. The notation $\Theta_{j,rs}$ refers to the r^{th} row and s^{th} column element in the parameter matrix $\Theta_{h,j,t}$ with different h in (a) and (b).

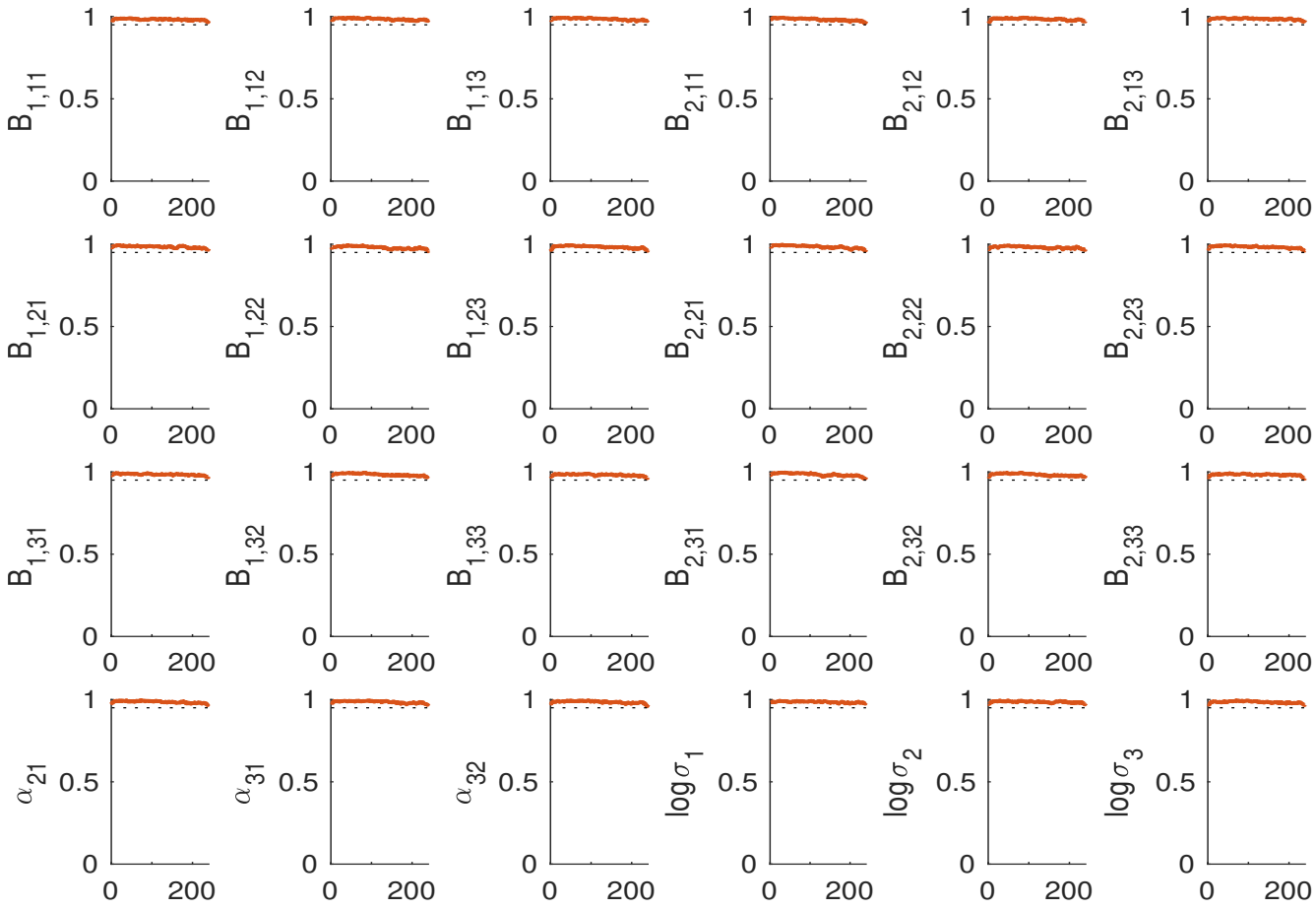

Figure 15: Coverage rates of TVP-VAR credible intervals, $T = 240$, $K = 3$, $p = 2$, $c = 1$, $C = \{0, 5, \cdots, 50\}$

Note: This figure plots the coverage rates of TVP-VAR credible intervals with $T = 240$, $K = 3$, $p = 2$, $c = 1$ across 2000 replications. $C = \{0, 5, \cdots, 50\}$ is considered in the estimation procedure. The black dotted line is the 95% horizontal line. The notation $B_{j,rs}, j = 1, 2$ refers to the r^{th} row and s^{th} column element in the parameter matrix $B_{j,t}, j = 1, 2$.

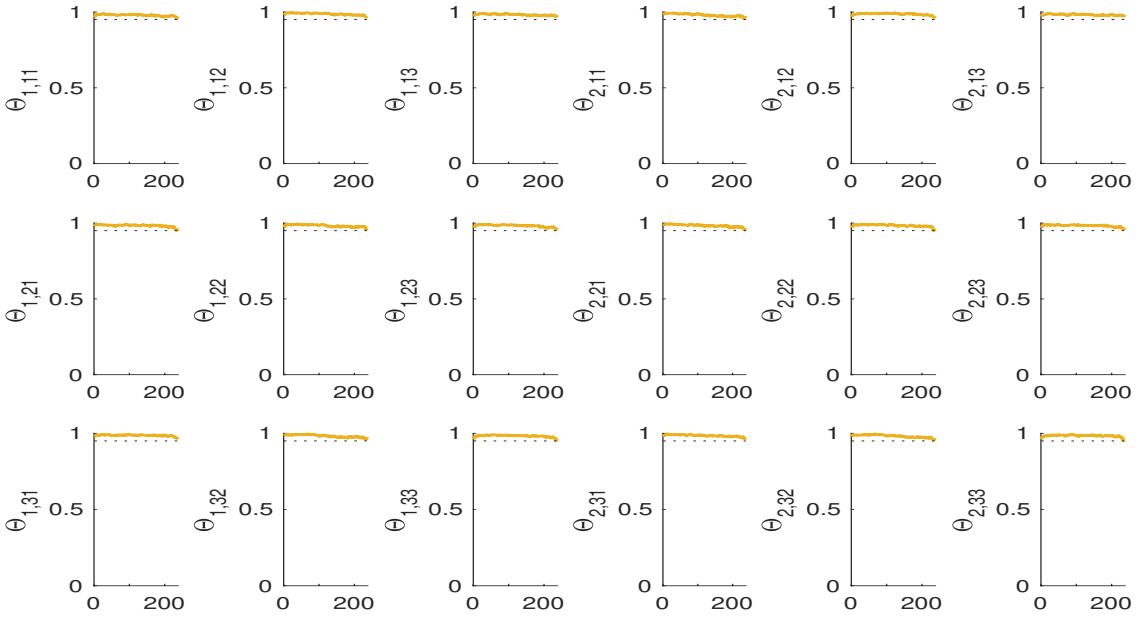

(a) $h = 2$

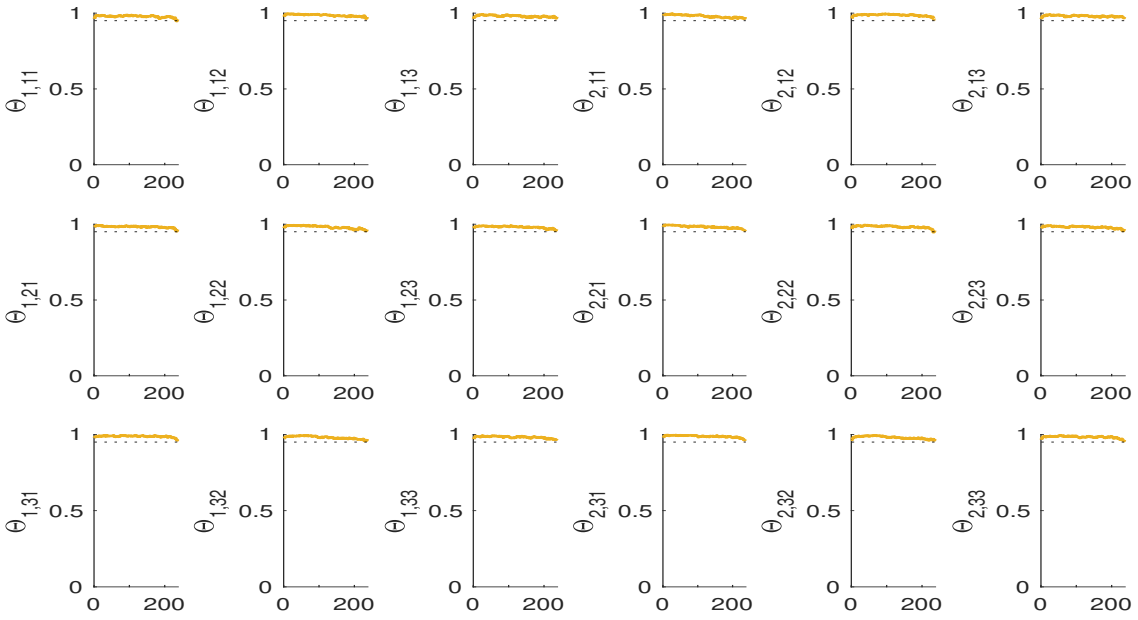

(b) $h = 3$

Figure 16: Coverage rates of TVP-LP credible intervals, $T = 240$, $K = 3$, $p = 2$, $c = 1$, $C = \{0, 5, \cdots, 50\}$

Note: This figure plots the coverage rates of TVP-LP credible intervals with $T = 240$, $K = 3$, $p = 2$, $c = 1$ across 2000 replications. $C = \{0, 5, \cdots, 50\}$ is considered in the estimation procedure. The black dotted line is the 95% horizontal line. The x-axis refers to the periods, and y-axis refers to the parameters where the subscripts h and t are omitted for notational simplicity. The notation $\Theta_{j,rs}$ refers to the r^{th} row and s^{th} column element in the parameter matrix $\Theta_{h,j,t}$ with different h in (a) and (b).

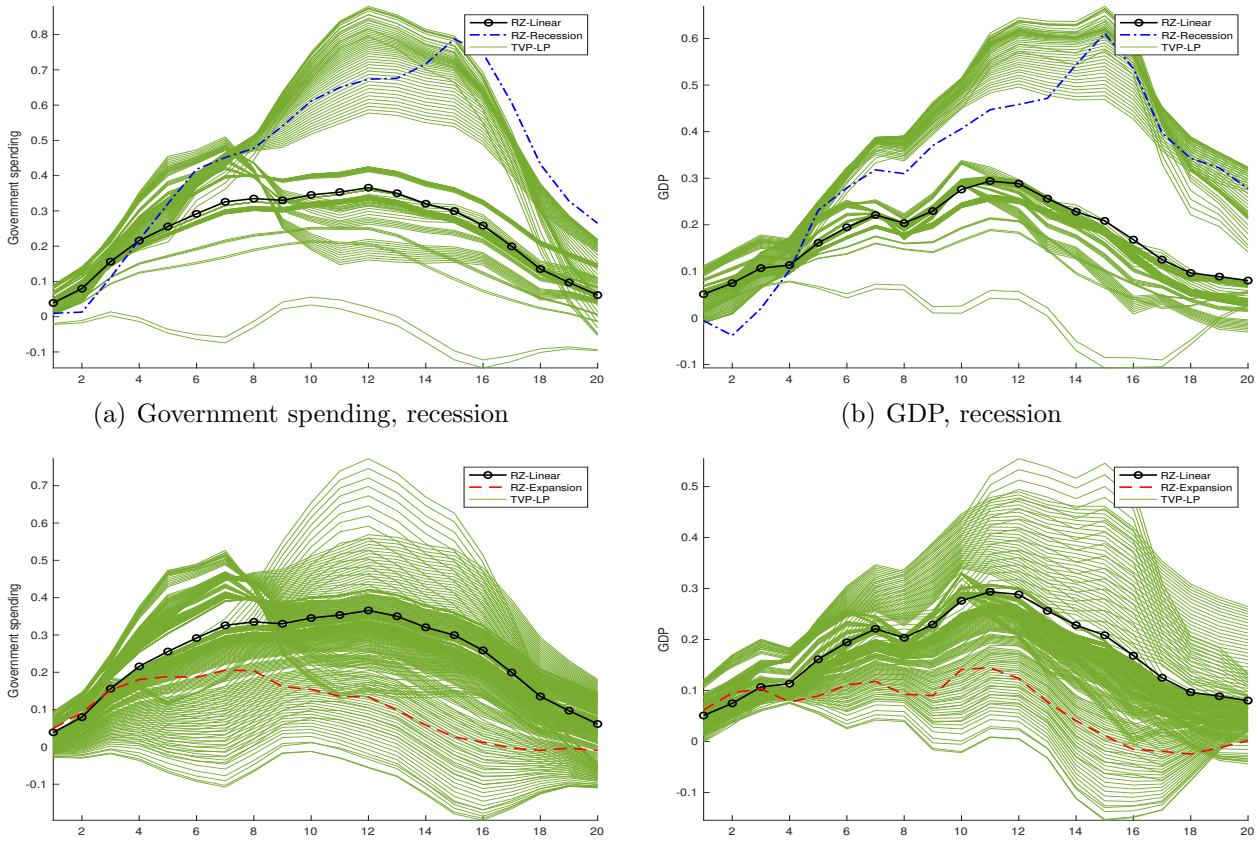

(a) Government spending, recession

(b) GDP, recession

(c) Government spending, expansion

(d) GDP, expansion

Figure 17: Government spending and GDP responses to a news shock

Note: This figure plots government spending and GDP responses to a Ramey and Zubairy (2018) military news shock equal to 1 percent of GDP. Each plot includes responses from Ramey and Zubairy's (2018) linear model (labeled 'RZ Linear') and state dependent model (labeled 'RZ-Expansion' and 'RZ-Recession'), where the state variable is unemployment, as well as responses based on TVP-LP path estimates at different periods classified in the corresponding states. The x-axis refers to horizons (quarters), and y-axis refers to the impulse responses of government spending and GDP, respectively.

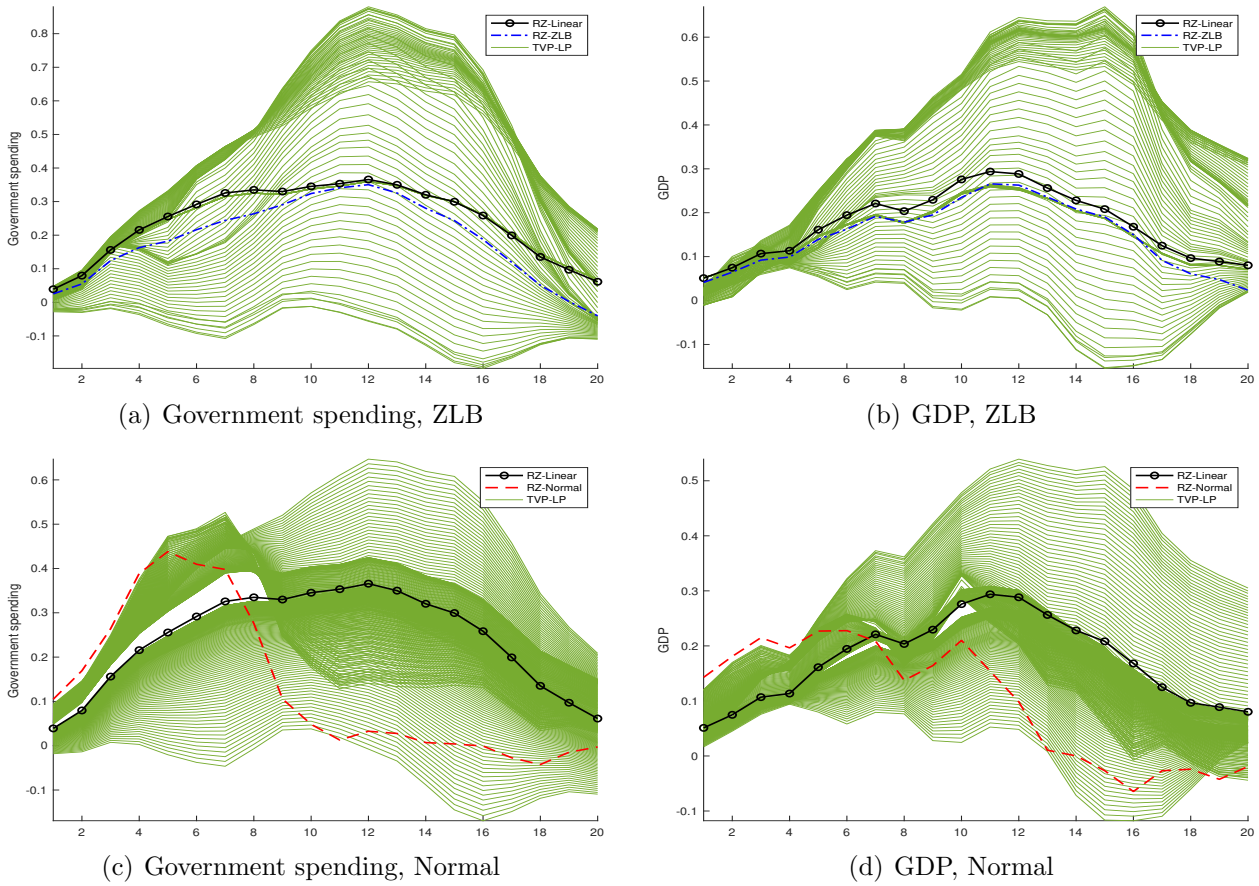

(a) Government spending, ZLB

(b) GDP, ZLB

(c) Government spending, Normal

(d) GDP, Normal

Figure 18: Government spending and GDP responses to a news shock

Note: This figure plots government spending and GDP responses to a Ramey and Zubairy (2018) military news shock equal to 1 percent of GDP. Each plot includes responses from Ramey and Zubairy's (2018) linear model (labeled 'RZ Linear') and state dependent model (labeled 'RZ-ZLB' and 'RZ-Normal'), where the state variable is ZLB, as well as responses based on TVP-LP path estimates at different periods classified in the corresponding states. The x-axis refers to horizons (quarters), and y-axis refers to the impulse responses of government spending and GDP, respectively.

Table 1: Estimates of Multipliers

	Linear	High u_t	Low u_t	ZLB	Normal	-	-	-	-
2-year	0.66	0.60	0.59	0.76	0.63	-	-	-	-
	(0.110)	(0.156)	(0.150)	(0.174)	(0.245)	-	-	-	-
4-year	0.71	0.68	0.67	0.75	0.78	-	-	-	-
	(0.072)	(0.086)	(0.199)	(0.095)	(0.619)	-	-	-	-
TVP-LP-IV						1938:Q1	1945:Q1	1954:Q1	1984:Q1
2-year	-	-	-	-	-	0.79	0.86	0.94	0.64
	-	-	-	-	-	(0.346)	(0.333)	(0.370)	(0.566)
4-year	-	-	-	-	-	0.84	0.81	0.84	0.69
	-	-	-	-	-	(0.304)	(0.317)	(0.283)	(0.428)

Note: This table reports 2/4-year integral multipliers with 90% confidence intervals from the Ramey and Zubairy (2018) linear model (labeled 'Linear'), the Ramey and Zubairy (2018) state-dependent model using unemployment or the ZLB as the state (labeled 'High u_t'/'Low u_t' and 'ZLB'/'Normal', respectively), as well as our TVP-LP-IV path estimates. The values in parentheses under the multipliers give the 90% confidence intervals. Note that, according to Ramey and Zubairy's (2018) state variables, 1938:Q1, 1945:Q1, 1954:Q1, 1984:Q1 are classified as "Recession, Expansion, Expansion, Recession", and "ZLB, ZLB, Normal, Normal", respectively.

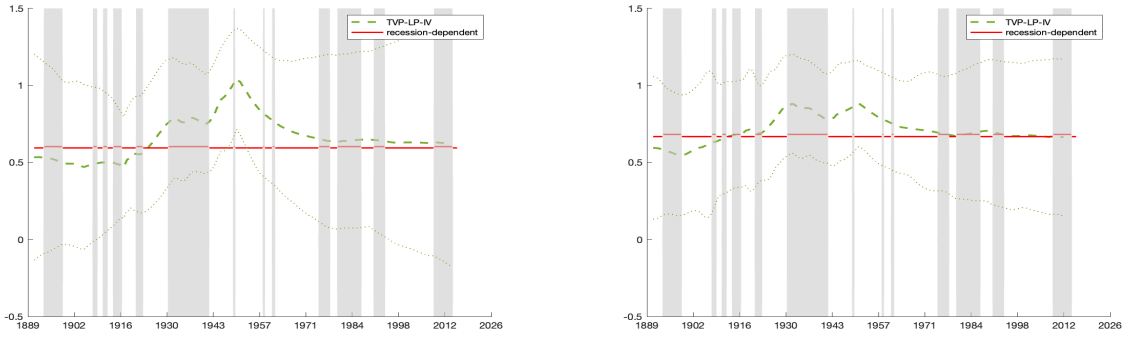

(a) 2-year integral

(b) 4-year integral

Figure 19: Cumulative spending multipliers across time, TVP-LP-IV estimates compared with recession-dependent results

Note: This figure plots 2/4-year integral multipliers from Ramey and Zubairy's (2018) state-dependent model where the state variable is unemployment (labeled 'recession-dependent'), as well as multipliers based on our TVP-LP-IV path estimates (labeled 'TVP-LP-IV') with 90% confidence intervals (green dotted lines). The shaded areas denote the recession periods (unemployment is above 6.5).

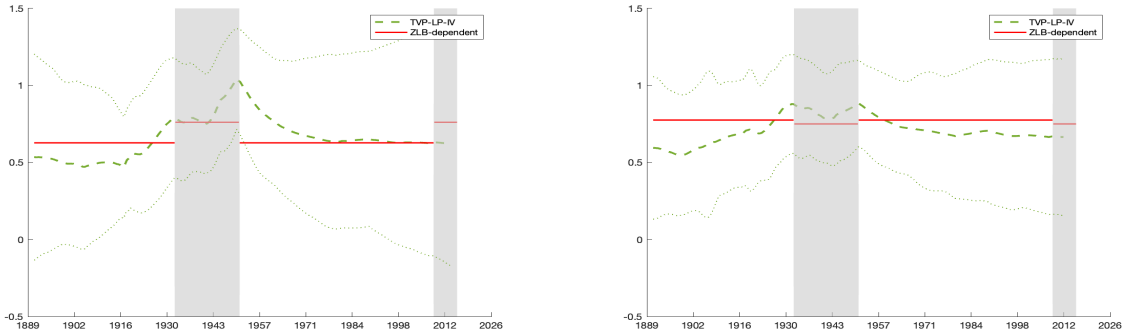

(a) 2-year integral

(b) 4-year integral

Figure 20: Cumulative spending multipliers across time, TVP-LP-IV estimates compared with ZLB-dependent results

Note: This figure plots 2/4-year integral multipliers from Ramey and Zubairy's (2018) state-dependent model where the state variable is ZLB (labeled 'ZLB-dependent'), as well as multipliers based on our TVP-LP-IV path estimates (labeled 'TVP-LP-IV') with 90% confidence intervals (green dotted lines). The shaded areas denote the ZLB periods.

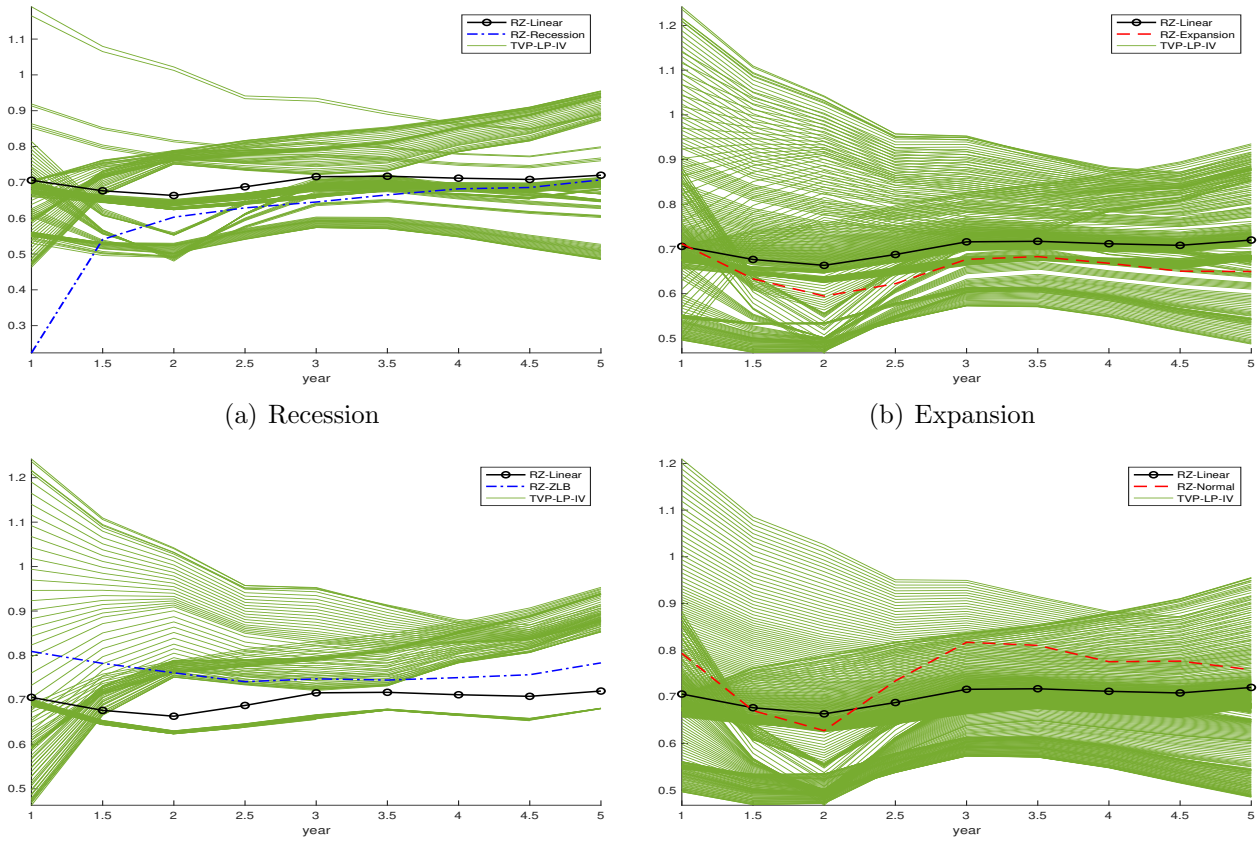

(a) Recession (b) Expansion

(c) ZLB (d) Normal

Figure 21: Cumulative spending multipliers across horizons

Note: This figure plots cumulative spending multipliers calculated across different horizons (years) during recessions/expansions or ZLB/Normal periods. Each plot includes multipliers based on the Ramey and Zubairy (2018) linear model and state-dependent (unemployment/ZLB-dependent) model, denoted as RZ-Linear/Recession/Expansion or RZ-Linear/ZLB/Normal, as well as multipliers based on our TVP-LP-IV path estimates at different periods classified in the corresponding states. The x-axis refers to years, and y-axis refers to the multipliers.

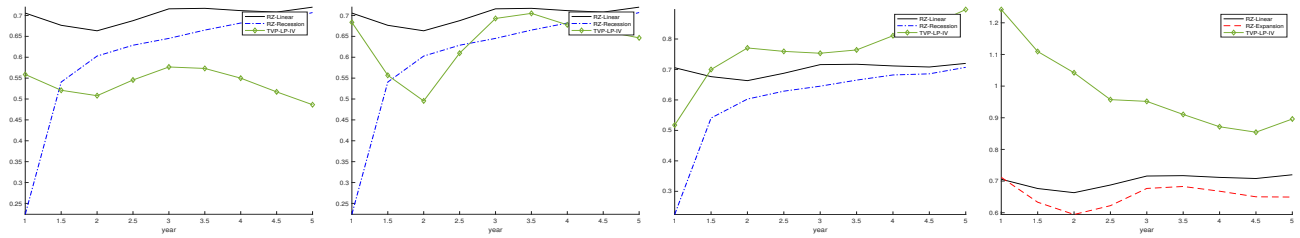

(a) 1898q1: The Spanish-American War starts with the sinking of the USS Maine.

(b) 1914q3: WWI starts

(c) 1939q3: WWII starts

(d) 1950q3: Korean War starts

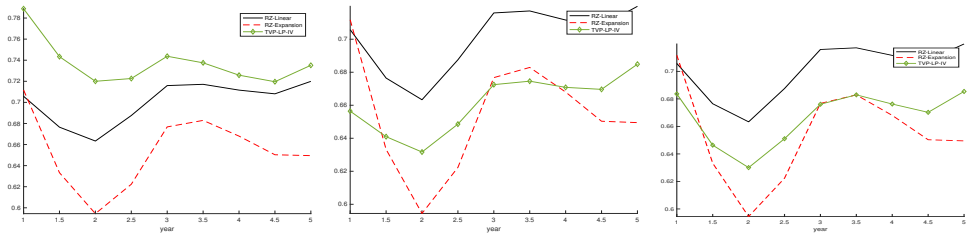

(e) 1965q1: Vietnam War starts

(f) 1980q1: Buildup in response to Soviet invasion of Afghanistan

(g) 2001q3: 9/11

Figure 22: Cumulative spending multipliers at war dates

Note: This figure plots multipliers across different horizons (years) at various war dates. Each plot includes multipliers from Ramey and Zubairy's (2018) linear model (labeled 'RZ Linear') and state-dependent model where the state variable is unemployment (labeled 'RZ-Recession' or 'RZ-Expansion'), as well as multipliers based on our TVP-LP-IV path estimates. The x-axis refers to years, and y-axis refers to the multipliers.

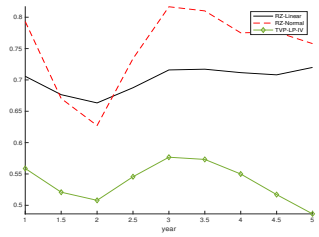

(a) 1898q1: The Spanish-American War starts with the sinking of the USS Maine.

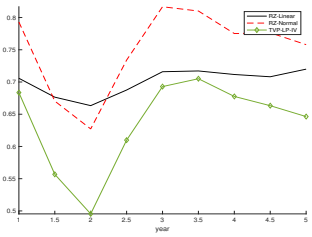

(b) 1914q3: WWI starts

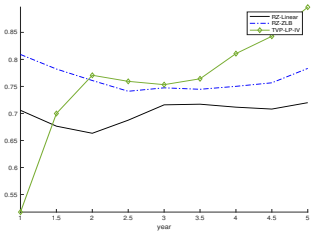

(c) 1939q3: WWII starts

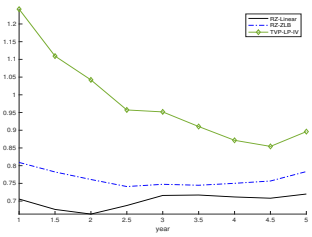

(d) 1950q3: Korean War starts

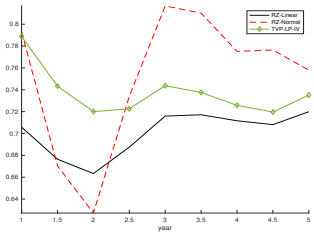

(e) 1965q1: Vietnam War starts

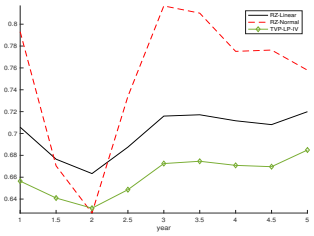

(f) 1980q1: Buildup in response to Soviet invasion of Afghanistan

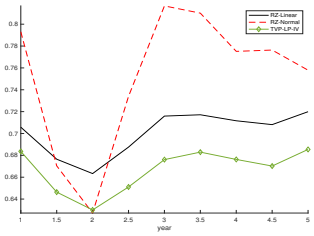

(g) 2001q3: 9/11

Figure 23: Cumulative spending multipliers across horizons at war dates

Note: This figure plots multipliers across different horizons at various war dates. Each plot includes multipliers from Ramey and Zubairy's (2018) linear model (labeled 'RZ Linear') and state-dependent model where the state variable is ZLB (labeled 'RZ-ZLB' or 'RZ-Normal'), as well as multipliers based on our TVP-LP-IV path estimates. The x-axis refers to years, and y-axis refers to the multipliers.

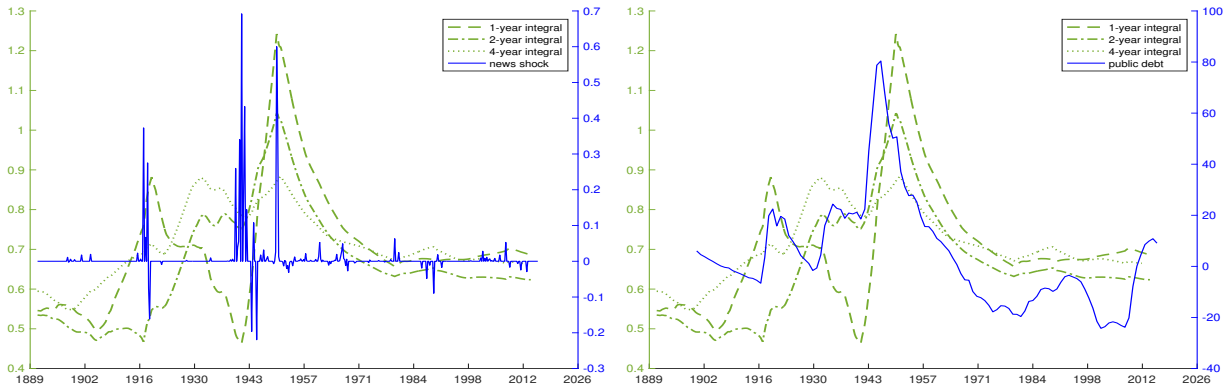

(a) (b)

Figure 24: Cumulative spending multipliers across time

Note: Figure (a) plots 1/2/4-year integral multipliers based on our TVP-LP-IV path estimates (labeled '1/2/4-year integral', with y-axis on the left) across time, together with the news shock (labeled 'news shock', with y-axis on the right). Figure (b) plots 1/2/4-year integral multipliers based on our TVP-LP-IV path estimates (labeled '1/2/4-year integral', with y-axis on the left) across time, together with the detrended public debt (labeled 'public debt', with y-axis on the right).

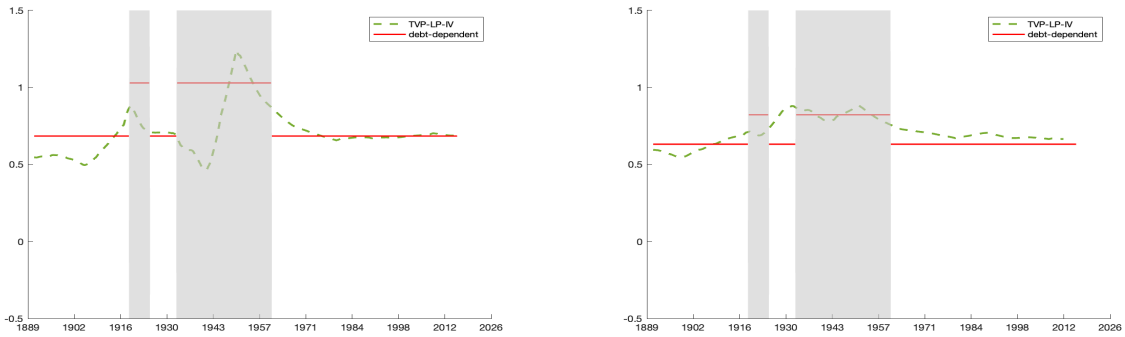

(a) 1-year integral (b) 4-year integral

Figure 25: Cumulative spending multipliers across time, TVP-LP-IV estimates compared with public debt-dependent results

Note: This figure plots 1/4-year integral multipliers from Ramey and Zubairy's (2018) state-dependent model where the state variable is public debt (labeled 'debt-dependent'), as well as multipliers based on our TVP-LP-IV path estimates (labeled 'TVP-LP-IV'). The shaded areas denote the periods when detrended public debt is above 11).

References

Auerbach, A. J. and Gorodnichenko, Y.: 2012, Measuring the output responses to fiscal policy, *American Economic Journal: Economic Policy* **4**(2), 1–27.

Barnichon, R. and Brownlees, C.: 2019, Impulse response estimation by smooth local projections, *Review of Economics and Statistics* **101**(3), 522–530.

Barnichon, R., Debortoli, D. and Matthes, C.: 2021, Understanding the size of the government spending multiplier: it's in the sign, *Review of Economic Studies, Forthcoming* .

Blanchard, O. and Perotti, R.: 2002, An empirical characterization of the dynamic effects of changes in government spending and taxes on output, *the Quarterly Journal of Economics* **117**(4), 1329–1368.

Caggiano, G., Castelnuovo, E., Colombo, V. and Nodari, G.: 2015, Estimating fiscal multipliers: News from a non-linear world, *The Economic Journal* **125**(584), 746–776.

Canova, F.: 1993, Modelling and forecasting exchange rates with a bayesian time-varying coefficient model, *Journal of Economic Dynamics and Control* **17**(1-2), 233–261.

Clark, T. E.: 2011, Real-time density forecasts from bayesian vector autoregressions with stochastic volatility, *Journal of Business & Economic Statistics* **29**(3), 327–341.

Cloyne, J. S., Jordà, Ò. and Taylor, A. M.: 2021, Decomposing the fiscal multiplier.

Cogley, T. and Sargent, T. J.: 2005, Drifts and volatilities: monetary policies and outcomes in the post WWII US, *Review of Economic Dynamics* **8**(2), 262–302.

Elliott, G. and Müller, U. K.: 2006, Efficient tests for general persistent time variation in regression coefficients, *The Review of Economic Studies* **73**(4), 907–940.

Fazzari, S. M., Morley, J. and Panovska, I.: 2015, State-dependent effects of fiscal policy, *Studies in Nonlinear Dynamics & Econometrics* **19**(3), 285–315.

Fazzari, S. M., Morley, J. and Panovska, I.: 2021, When is discretionary fiscal policy effective?, *Studies in Nonlinear Dynamics & Econometrics* **25**(4), 229–254.

Goemans, P.: 2022, Historical evidence for larger government spending multipliers in uncertain times than in slumps, *Economic Inquiry* .

Inoue, A. and Rossi, B.: 2011, Identifying the sources of instabilities in macroeconomic fluctuations, *Review of Economics and Statistics* **93**(4), 1186–1204.

Jordà, Ò.: 2005, Estimation and inference of impulse responses by local projections, *American Economic Review* **95**(1), 161–182.

Jordà, Ò.: 2020, Local projections: new developments, *mimeo* .

Kendrick, J. W.: 1961, *Productivity trends in the United States*, number kend61-1, National Bureau of Economic Research.

Levine, D.: 1983, A remark on serial correlation in maximum likelihood, *Journal of Econometrics* **23**(3), 337–342.

Lusompa, A.: 2021, Local projections, autocorrelation, and efficiency, *Federal Reserve Bank of Kansas City Working Paper* (21-01).

Miranda-Agrippino, S. and Ricco, G.: 2021, The transmission of monetary policy shocks, *American Economic Journal: Macroeconomics* **13**(3), 74–107.

Montiel Olea, J. L. and Plagborg-Møller, M.: 2021, Local projection inference is simpler and more robust than you think, *Econometrica* **89**(4), 1789–1823.

Montiel Olea, J. L., Stock, J. H. and Watson, M. W.: 2021, Inference in structural vector autoregressions identified with an external instrument, *Journal of Econometrics* **225**(1), 74–87.

Müller, U. K.: 2013, Risk of bayesian inference in misspecified models, and the sandwich covariance matrix, *Econometrica* **81**(5), 1805–1849.

Müller, U. K. and Petalas, P.-E.: 2010, Efficient estimation of the parameter path in unstable time series models, *The Review of Economic Studies* **77**(4), 1508–1539.

Mumtaz, H. and Petrova, K.: 2018, Changing impact of shocks: a time-varying proxy svar approach.

Newey, W. K. and West, K. D.: 1987, A simple, positive semi-definite, heteroskedasticity and autocorrelationconsistent covariance matrix, *Econometrica* **55**, 703–708.

Owyang, M. T., Ramey, V. A. and Zubairy, S.: 2013, Are government spending multipliers greater during periods of slack? evidence from twentieth-century historical data, *American Economic Review* **103**(3), 129–34.

Plagborg-Møller, M. and Wolf, C. K.: 2021, Local projections and vars estimate the same impulse responses, *Econometrica* **89**(2), 955–980.

Primiceri, G. E.: 2005, Time varying structural vector autoregressions and monetary policy, *The Review of Economic Studies* **72**(3), 821–852.

Ramey, V. A.: 2011a, Can government purchases stimulate the economy?, *Journal of Economic Literature* **49**(3), 673–85.

Ramey, V. A.: 2011b, Identifying government spending shocks: It's all in the timing, *The Quarterly Journal of Economics* **126**(1), 1–50.

Ramey, V. A. and Zubairy, S.: 2018, Government spending multipliers in good times and in bad: evidence from us historical data, *Journal of Political Economy* **126**(2), 850–901.

Rossi, B. and Zubairy, S.: 2011, What is the importance of monetary and fiscal shocks in explaining us macroeconomic fluctuations?, *Journal of Money, Credit and Banking* **43**(6), 1247–1270.

Ruisi, G.: 2019, Time-varying local projections.

Sims, C. A.: 1980, Macroeconomics and reality, *Econometrica: Journal of the Econometric Society* pp. 1–48.

Stock, J. H. and Watson, M. W.: 2001, Vector autoregressions, *Journal of Economic Perspectives* **15**(4), 101–115.

Stock, J. H. and Watson, M. W.: 2016, Dynamic factor models, factor-augmented vector autoregressions, and structural vector autoregressions in macroeconomics, *Handbook of Macroeconomics*, Vol. 2, Elsevier, pp. 415–525.

Stock, J. H. and Watson, M. W.: 2018, Identification and estimation of dynamic causal effects in macroeconomics using external instruments, *The Economic Journal* **128**(610), 917–948.

White, H.: 1982, Maximum likelihood estimation of misspecified models, *Econometrica: Journal of the Econometric Society* pp. 1–25.